Osteology of *Batrachuperus londongensis* (Urodela, Hynobiidae): study of bony anatomy of a facultatively neotenic salamander from Mount Emei, Sichuan Province, China

Jian-ping Jiang [1] , **Jia Jia** [2] , **Meihua Zhang** [1] , **Ke-Qin Gao** Corresp. [2]

[1] Chengdu Institute of Biology, Chinese Academy of Sciences, Chengdu, China

[2] School of Earth and Space Sciences, Peking University, Beijing, China

Corresponding Author: Ke-Qin Gao
Email address: kqgao@pku.edu.cn

The Longdong Stream Salamander *Batrachuperus londongensis*, living in a mountain stream environment at Mt. Emei in Sichuan Province, China, represents a rare species that is facultatively neotenic in the family Hynobiidae. Although the species has been known to science for some 40 years since its initial discovery in the late 1970s, anatomical details of its osteology remain poorly understood and developmental information is still lacking for the species. This study 1) provides a detailed osteological account of *B. londongensis* based on micro-CT scanning and clearing and staining of multiple specimens from the type locality; 2) provides a discussion of intraspecific variation related to life-history differences; and 3) presents a discussion on limb features related to morphological evolution of limb patterns correlative with ecological adaptation to mountain stream environments. Osteological comparisons with congeneric species has led to recognition of several diagnostic features that are unique to *B. londongensis*, including: vomers widely separated from one another, lacking a midline contact; presence of uncommon perichondral ossification of the ascending process of the palatoquadrate as part of the suspensorium; and presence of a prominent posterodorsal process of the scapular blade, which serves as a ligamentous insertion of the levator muscle of the scapula. In addition, some but not all neotenic individuals retain the palatine as a discrete element, indicative of its delayed absorption after sexual maturity. Postmetamorphic and neotenic individuals are strikingly different in the complexity of hyobranchial structures. Neotenes display a high degree of ossification of hyobranchial elements, tend to increase ossification of both hypobranchial I and ceratobranchial I during aging, and retain fully ossified ceratobranchial III and IV; in contrast, these elements remain entirely cartilaginous or are totally lost by resorption in postmetamorphic individuals. In addition, all postmetamorphic forms display an inverted "T"-shaped basibranchial II, whereas neotenes show transformation from a "fork"-shaped

to the "T"-shaped configuration after sexual maturity. *Batrachuperus londongensis* displays a mosaic of apomorphic and plesiomorphic states in its limb ossifications: presence of a single centrale element in both the manus and pes is a derived condition in Hynobiidae and other families as well, whereas retention of a postminimus in the pes is obviously plesiomorphic within Urodela. Reduction in number of digits from five to four in the pes and possession of a cornified sheath covering the terminal phalanges are also derived features shared with some but not all mountain stream salamanders that are adapted to a similar type of environment.

Osteology of *Batrachuperus londongensis* (Urodela,

Hynobiidae): study of bony anatomy of a facultatively

neotenic salamander from Mount Emei, Sichuan Province,

China

7 Jian-ping Jiang[1], Jia Jia[2], Meihua Zhang[1], Ke-Qin Gao[2]

8 [1]Chengdu Institute of Biology, Chinese Academy of Sciences, Chengdu 610041, China

9 [2]School of Earth and Space Sciences, Peking University, Beijing 100871, China

12 Corresponding authors: Ke-Qin Gao, 5 Yiheyuan Road, Beijing 100871, China

13 Email address: kqgao@pku.edu.cn

Abstract

18 The Longdong Stream Salamander *Batrachuperus londongensis*, living in a mountain stream

19 environment at Mt. Emei in Sichuan Province, China, represents a rare species that is

20 facultatively neotenic in the family Hynobiidae. Although the species has been known to science

21 for some 40 years since its initial discovery in the late 1970s, anatomical details of its osteology

22 remain poorly understood and developmental information is still lacking for the species. This

23 study 1) provides a detailed osteological account of *B. londongensis* based on micro-CT scanning

24 and clearing and staining of multiple specimens from the type locality; 2) provides a discussion

25 of intraspecific variation related to life-history differences; and 3) presents a discussion on limb

26 features related to morphological evolution of limb patterns correlative with ecological

27 adaptation to mountain stream environments. Osteological comparisons with congeneric species

28 has led to recognition of several diagnostic features that are unique to *B. londongensis*, including:

29 vomers widely separated from one another, lacking a midline contact; presence of uncommon

30 perichondral ossification of the ascending process of the palatoquadrate as part of the

31 suspensorium; and presence of a prominent posterodorsal process of the scapular blade, which

32 serves as a ligamentous insertion of the levator muscle of the scapula. In addition, some but not

33 all neotenic individuals retain the palatine as a discrete element, indicative of its delayed

34 absorption after sexual maturity. Postmetamorphic and neotenic individuals are strikingly

35 different in the complexity of hyobranchial structures. Neotenes display a high degree of

36 ossification of hyobranchial elements, tend to increase ossification of both hypobranchial I and

37 ceratobranchial I during aging, and retain fully ossified ceratobranchial III and IV; in contrast,

38 these elements remain entirely cartilaginous or are totally lost by resorption in postmetamorphic

39   individuals. In addition, all postmetamorphic forms display an inverted "T"-shaped

40   basibranchial II, whereas neotenes show transformation from a "fork"-shaped to the "T"-shaped

41   configuration after sexual maturity. *Batrachuperus londongensis* displays a mosaic of

42   apomorphic and plesiomorphic states in its limb ossifications: presence of a single centrale

43   element in both the manus and pes is a derived condition in Hynobiidae and other families as

44   well, whereas retention of a postminimus in the pes is obviously plesiomorphic within Urodela.

45   Reduction in number of digits from five to four in the pes and possession of a cornified sheath

46   covering the terminal phalanges are also derived features shared with some but not all mountain

47   stream salamanders that are adapted to a similar type of environment.

Introduction

50   The family Hynobiidae includes 66–67 species in 9–11 genera (Fei et al., 2006; AmphibiaWeb,

51   2017; Frost, 2017). These are small to medium sized salamanders found primarily in Asia,

52   although geographical range of one species (the Siberian Salamander *Salamandrella*

53   *keyserlingii*) extends from Asia into European Russia (AmphibiaWeb, 2017; Frost, 2017).

54   Phylogenetically, the Hynobiidae form the sister clade with Cryptobranchidae, the two families

55   together classified in the suborder Cryptobranchoidea Dunn, 1922. The Hynobiidae have long

56   been viewed as a group of primitive salamanders, as they lack derived features such as fusion of

57   the angular with the prearticular in the lower jaw, but retain plesiomorphic features, including

58   external fertilization (Dunn, 1923; Noble, 1931), a large number of chromosomes (2n= 40–78),

59   and the presence of microchromosomes (Morescalchi, 1973, 1975; Edwards, 1976; Sessions,

60   2008).

61   Based on the fossil record from northern China, the evolutionary history of the

62 Hynobiidae can be traced back to Aptian time (~125 Ma) during the Early Cretaceous (Chen &

63 Gao, 2009; Gao, Chen & Jia, 2013; Jia & Gao, 2016b). Several extinct taxa from China

64 including *Liaoxitriton* and *Nuominerpeton* are apparently stem-group hynobiids, as evidenced by

65 their possession of derived features shared with extant hynobiids, including: transverse and

66 arched vomerine tooth rows; a deeply notched posterolateral border of the vomer for choana; and

67 an optic foramen opening at the notched posterior border of orbitosphenoid (Chen & Gao, 2009;

68 Gao, Chen & Jia, 2013; Jia & Gao, 2016a). The fossil record indicates that the split of the

69 hynobiid from cryptobranchid clade seems to be a phylogenetic event that had taken place no

70 later than the Aptian time (~125 Ma). Recent analyses of the nuclear exon and mitochondrial

71 genome estimate the Cryptobranchidae-Hynobiidae split as ~150 Ma and the origin of crown-

72 group hynobiids as ~125 Ma (Zheng et al., 2011: fig. 3). A more recent analysis of nuclear

73 genes, however, yielded an estimate of ~157 Ma for the split and ~135 Ma for the origin of

74 crown-group hynobiids (Chen et al., 2015: fig. 2).

75   Most hynobiids are terrestrial in the adult stage, but species in several genera

76 (*Batrachuperus*, *Liua*, *Pachyhynobius*, *Ranodon* and *Paradactylodon*) are mostly mountain

77 stream dwellers that can be found in water all year around (Reilly, 1983; Fei et al., 2006;

78 Sparreboom, 2014; AmphibiaWeb, 2017). In terms of life-history features, most hynobiids have

79 a biphasic life cycle, with a gilled aquatic larval stage going through metamorphosis to a

80 postmetamorphic adult stage. The exception is the Japanese species *Hynobius retardatus*, which

81 has been reported as partly neotenic as a population variant from Lake Kuttarush in Hokkaido,

82 with some specimens reaching a total length of 150 mm while retaining gills (Sasaki, 1924).

83 However, this population now appears to be extinct, with no osteological description of the

84 population ever undertaken (Inukai, 1930–1932; Wakahara, 1996). Accordingly, *Batrachuperus*

85   *londongensis* Liu & Tian, 1978, commonly known as the Longdong Stream Salamander, appears

86   to be the only extant hynobiid species that has been documented as facultatively neotenic (Fei et

87   al., 2006). Osteological study of this unusual hynobiid is bound to be significant for

88   understanding patterns of ossification of the cranium and post-cranium, and for reconstruction of

89   the evolution of hynobiid salamanders more generally. Furthermore, such an osteological study

90   is in urgent need because survival of the species at the type locality Longdong Stream is facing a

91   severe threat from habitat destruction and illegal collection (see below).

92   Within Hynobiidae, the genus *Batrachuperus* includes six or seven species (Fei et al.,

93   2006; Fu & Zeng, 2008; Fei, Ye & Jiang, 2010) that are all endemic to western China. The

94   genus consists of the type species *Batrachuperus pinchonii* (David, 1872) plus five other species

95   (*B. londongensis*, *B. tibetanus*, *B. yenyuanensis*, *B. taibaiensis*, and *B. karlschmidti*; see Fei et al.,

96   2006; Fu & Zeng, 2008). Another nominal taxon, *Batrachuperus cochranae* Liu, 1950, was

97   synonymized with *Batrachuperus pinchonii* based on molecular evidence (Fu & Zeng, 2008), but

98   the validity of the name is still in dispute (Fei, Ye & Jiang, 2010, 2012). All of these are aquatic

99   forms that inhabit mountain stream and/or plateau pond environments, at elevations ranging from

100 1200 m–4400 m above sea level (Fei et al., 2006; Fei, Ye & Jiang, 2010). In terms of

101 conservation status, most of these species are currently vulnerable (Jiang et al., 2016).   No

102 fossil record has been found for *Batrachuperus* or its sister clade (*Liua + Pseudohynobius*).

103 Based on molecular data alone, *Batrachuperus* was estimated as having originated in the late

104 Miocene (~7.3 Ma) in a recent analysis using 29 nuclear genes (Chen et al., 2015), a much

105 younger date than the estimation of ~24.3 Ma based on the complete mitochondrial genome

106 (Zhang et al., 2006) or that of 20–30 Ma based on complete mitochondrial genome and three

107 nuclear genes (Zheng et al., 2011).

108   *Batrachuperus* is one of the several hynobiid genera (*Batrachuperus*, *Liua*,

109   *Pachyhynobius*, *Paradactylodon, Pseudohynobius*) that have received little study of their

110   developmental osteology (Rose, 2003); moreover, anatomical details remain poorly known for

111   these taxa. For the genus *Batrachuperus*, brief osteological accounts of the type species, *B.*

112   *pinchonii* can be found in the literature (e.g., Zhang et al., 2009; Xiong et al., 2013a); however,

113   adequate osteological description of *B. londongensis* is still lacking, although the species has

114   been known to science for almost 40 years since its discovery in the late 1970s. In regard to

115   phylogenetic relationships, few adequate data can be found in the literature on osteological

116   details of the species. Attempting to improve this awkward situation, our study provides a

117   detailed osteological account of *B. londongensis* and a morphological comparison in relation to

118   life-history differences within this species; in addition, we present a discussion on diagnosis of

119   the species based on bony features, patterns of ossification of the hyobranchium and limb

120   ossification. Phylogenetic analysis will be performed in future research when necessary data

121   becomes available for other congeneric species.

122

123   Materials & Methods

124   A total of 12 specimens of *Batrachuperus londongensis* were used in this study, including both

125   juvenile (1) and adults (11), and both postmetamorphic (4) and neotenic (8) individuals (Table

126   1). The material used includes both dry skeletons and fluid-preserved (10% formaldehyde)

127   specimens. In addition, cleared and stained specimens (CIB 14499, 14504) allowed observation

128   of both bony and cartilaginous structures. All of these specimens are deposited in the Chengdu

129   Institute of Biology (CIB), Chinese Academy of Sciences, Chengdu, China. For purpose of

130   comparison, several specimens belonging to congeneric species and other hynobiid species were

131   used in this study (see Table S1).

132   Total length (TL) refers to the measurement between the tip of the snout and the posterior

133   extremity of the tail; snout–pelvic length (SPL) is the measurement from the tip of the snout to

134   the posterior end of the pelvis (marked by the anus in fluid-preserved specimens and by the

135   haemal arch of the last caudosacral in dry skeletons). Skull length (SKL) refers to the maximum

136   dimension from the tip of the snout to the posterior end of the occipital condyles; skull width

137   (SKW) is the distance measured between the cranio-mandibular joints. All measurements are in

138   millimeters (mm). Anatomical nomenclature follows Francis (1934), Reilly & Lauder (1988),

139   and Shubin & Wake (2003), with the exceptions as noted in several cases.

140   The type specimen of *Batrachuperus londongensis* is a large male, with a TL of 265 mm

141   and a SPL of 129 mm (Fig. 1). The specimen carries a field number CIB 65I0013 as in previous

142   publications (e.g., Fei, Ye & Tian, 1983; Fei et al., 2006), but it has been formally catalogued as

143   CIB 65I0013/14380 in specimen collections at the Chengdu Institute of Biology (Fig. 1). This

144   specimen represents a neotenic form as it retains gill slits and a larval type of hyobranchium (Fei,

145   Ye & Tian, 1983; Fei et al., 2006). The specimen was collected on March 23, 1965 from the

146   type locality, Longdong Stream at Mount Emei (Emeishan), at an elevation of 1300 m above sea

147   level as has been documented in the literature (Liu & Tian, 1978; Fei, Ye & Tian, 1983).

148   Subsequent collections of specimens were made in 2002, 2006, 2014, and 2016 from the same

149   mountain stream by field crews from the Chengdu Institute of Biology (CIB).

150   Selected specimens from the CIB collections (Table 1), including the holotype (CIB

151   65I0013/14380), were CT scanned using a high-resolution X-ray scanner (Quantum GX micro-

152   CT Imaging System, PerkinElmer®) at the Chengdu Institute of Biology (CIB), Chinese

153   Academy of Sciences. These specimens were scanned along the coronal axis at an image

154 resolution of 2000 X 2000. Comparative specimens from the FMNH collections were CT

155 scanned at the University of Chicago (PaleoCT Lab) using a dual tube X-ray scanner from GE.

156 Segmentation and three-dimensional reconstruction of the CT images were made by using VG

157 Studio Max 2.2 (Volume Graphics, Heidelberg, Germany).

158   Two specimens (CIB 14504, 14499) were whole-mount cleared and double stained after

159 being scanned. The clearing and staining procedures followed the protocols of Hanken &

160 Wassersug (1981). Cartilaginous elements were stained in blue using Alcian Blue 8GX and bony

161 structures were stained in red using Alizarin Red, and then were cleared in glycerin KOH

162 solution. Line drawings of skeletal structures were prepared using Adobe Photoshop® CS6

163 software, and are presented as text figures and supplementary figures (Supporting Information).

164

165 **Institutional abbreviations—CIB**, Chengdu Institute of Biology, Chinese Academy of

166 Sciences, Chengdu, China; **FMNH**, Field Museum of Natural History, Chicago, USA; **MVZ**,

167 Museum of Vertebrate Zoology, University of California, Berkeley, USA.

168

169 **Anatomical abbreviations—act**, acetabulum; **adf**, anterodorsal fenestra; **amf**, anteromedial

170 fenestra; **an**, angular; **ar**, articular; **at**, atlas; **bb,** basibranchial; **bc**, basale commune; **c**, centrale;

171 **cb**, ceratobranchial; **ch**, ceratohyal; **cor**, coracoid; **corn**, cornua; **crd**, crista dorsalis; **crv**, crista

172 ventralis; **dc**, distal carpal; **den**, dentary; **dt**, distal tarsal; **etr**, external trochanter; **fe**, femur; **ftr**,

173 femoral trochanter; **fi**, fibula; **fib**, fibulare; **fr**, frontal; **glf**, glenoid fossa; **hb**, hypobranchial; **hu**,

174 humerus; **i**, intermedium; **icf**, internal carotid foramen; **il**, ilium; **isc**, ischium; **lac**, lacrimal; **lacf**,

175 lacrimal foramen; **mx**, maxilla; **na**, nasal; **obf**, obturator foramen; **obs**, orbitosphenoid; **op-ex**,

176 opisthotic-exoccipital complex; **pa**, parietal; **pcor**, procoracoid; **pm**, premaxilla; **po**,

177   postminimus; **pra**, prearticular; **prf**, prefrontal; **pro**, prootic; **ps**, parasphenoid; **pt**, pterygoid;

178   **pub**, pubis; **qu**, quadrate; **ra**, radius; **rad**, radiale; **rl**, radial loop; **sca**, scapulocoracoid; **scof**,

179   supracoracoid foramen; **sm**, septomaxilla; **sq**, squamosal; **st**, stapes; **stf**, stapedial foramen; **ti**,

180   tibia; **tib**, tibiale; **ul**, ulna; **uln**, ulnare; **vo**, vomer; **y**, element y; **yps**, ypsiloid.

181

182   ## Results

183   ### Systematics & Description

184   Order Urodela Duméril, 1806

185   Suborder Cryptobranchoidea Dunn, 1922

186   Family Hynobiidae Cope, 1859

187   Genus *Batrachuperus* Boulenger, 1878

188

189   Species *Batrachuperus londongensis* Liu & Tian, 1978

190

191   **Holotype**. CIB 65I0013/14380, a male adult with a total length of 265 mm, a snout-vent length

192   of 129 mm. The holotype is a neotenic individual, as it is sexually mature but retains gill slits

193   and a larval type of hyobranchium.

194   **Type locality**. Longdong Stream (N29°34'42.85"/E103°17'5.61"), at an elevation of 1300 m

195   above sea level, Mt. Emei (Emeishan), Sichuan Province, China.

196   **Known distribution and habitat**. The species was previously thought to be known only from

197   Longdong Stream, a mountain stream associated with the Longdong Cave at 1200 m–1300 m

198   above sea level (Fei et al., 2006); however, a molecular systematics study has shown that

199   populations previously identified as *B. pinchonii* from the nearby Mt. Wawushan in Hongya

200   County and Mt. Nibashan in Hanyuan County may pertain to *B. londongensis* (Fu & Zeng,

201   2008). Based on field observations at the type locality, live individuals of the Longdong Stream

202   Salamander often hide under rock cover in the mountain stream, and they feed on fresh-water

203   shrimp, aquatic insects and insect larvae (Fei, Ye & Jiang, 2010).

204   **Diagnosis**. *Batrachuperus londongensis* can be distinguished from the type species *B. pinchonii*

205   and all other congeneric species in having a unique combination of the following osteological

206   features: alary process of premaxilla barely contributing to border of anterodorsal fenestra

207   (shared with *B. tibetanus*); suture between nasal and frontal located at the level of anterior border

208   of orbit; frontal extending far posteriorly, terminating at the level of otic process of pterygoid;

209   vomers widely separated from one another, lacking a midline contact (unique); vomerine teeth

210   four to eight in number, arranged in a straight line that is strongly oblique and nearly vertical in

211   orientation (unique); ascending process of palatoquadrate ossified as a short pillar propping

212   lateral edge of parietal behind orbit (shared with *B. karlschmidti* and *B. taibaiensis*); radial loops

213   stemming from basibranchial I not crossing one another; presacral vertebrae 18 in number;

214   scapular blade bearing prominent posterodorsal process, onto which a levator muscle of the

215   scapula inserts (unique); ischial plate is penetrated by a small nerve foramen, and the ischial

216   spine is clearly more elongated than in other species.

217   **Taxonomic remarks**. In the literature, the species epithet has been confusingly spelled as

218   *Batrachuperus londongensis* (e.g., Liu & Tian, 1978; Liu et al., 1978; Fu et al., 2001; Wu & Xie,

219   2004; Fei et al., 2006; Fei, Ye & Jiang, 2010, 2012) and *Batrachuperus longdongensis* (e.g., Liu

220   & Tian, 1983 in Fei, Ye & Tian, 1983; Fei & Ye, 1984; Song et al., 2001). Judging from the

221   published literature regarding the two available names differing in spelling, it is clear that the

222   former is valid and the latter invalid owing to its status as a "nomen nudum" (Fei et al., 2006).

223   The validity of the species name *Batrachuperus londongensis* was established by Liu &

224   Tian (1978) in Liu et al. (1978). The year before this publication, the same authors (Liu & Tian,

225   1977) first published the species name spelled as "*Batrachuperus longdongensis*" in a systematic

226   checklist of Chinese amphibians (Laboratory of Amphibians and Reptiles, Biological Institute of

227   Sichuan Province, 1977) without a type designation, description, or illustration (see ICZN, 1999:

228   art. 13); for that reason, the name "*Batrachuperus longdongensis*" Liu & Tian, 1977 is

229   considered a nomen nudum (Fei et al., 2006). Unfortunately, Liu & Tian (1983, in Fei, Ye &

230   Tian, 1983) "re-published" the invalid name "*Batrachuperus longdongensis*" and labeled it as a

231   new species. Although the latter publication provided some detailed information on the species,

232   "*Batrachuperus longdongensis*" Liu & Tian 1983 cannot be considered as the original spelling,

233   but is a junior homonym of the nomen nudum "*Batrachuperus longdongensis*" Liu & Tian 1977.

234   Fei et al. (2006) evidently chose to adopt *Batrachuperus londongensis* as the original spelling in

235   a valid publication by Liu & Tian (1978). Moreover, the species name *Batrachuperus*

236   *londongensis* is in prevailing usage in the current literature (e.g., Fei et al., 2006; Fei & Ye,

237   2017; Fu & Zeng, 2008; Fei, Ye & Jiang, 2010, 2012; AmphibiaWeb, 2017; Frost, 2017; IUCN,

238   2016).

239

240   **External morphology**

241   Formalin-preserved specimens provide information on external morphology except for

242   coloration. Male adults of *Batrachuperus londongensis* have been measured at 190 mm–265 mm

243   in total length, and female adults at 183 mm–232 mm (Fei et al., 2006). Labial folds are well

244   developed, partly covering the lower lips; gular folds are arched posteriorly to demarcate the

245   head from the trunk. Neotenes have one to four pairs of gill slits, whereas in postmetamorphic

246   individuals the gill slits are closed.

247   The presence or absence of eyelids and ring-shaped scleral cartilages in the eye are both

248   ontogenetically and ecologically significant characters. Movable eyelids are normally developed

249   at metamorphosis for adult life on land, but are often lacking in larvae and in those adults that are

250   obligate neotenes (Duellman & Trueb, 1986). However, the ring-shaped scleral cartilage is

251   partly resorbed at metamorphosis in *Hynobius* and *Onychodactylus* (Okajima & Tsuaki, 1921),

252   while the extent of resorption of the scleral cartilage in other hynobiids is largely unknown

253   (Rose, 2003). Our observations indicate that *Batrachuperus londongensis* has movable eyelids

254   but lacks scleral cartilages in both neotenes and postmetamorphic individuals. Although

255   developmental information is still unavailable, we infer that it is likely that scleral cartilages are

256   fully resorbed at metamorphosis or at sexual maturity as a normal developmental pattern as in

257   other hynobiids. Because the species is facultatively rather than obligately neotenic, possession

258   of movable eyelids may be indicative of their all-season aquatic life style being a secondary

259   adaptation.

260   The trunk region is more or less cylindrical, having 12–14 costal grooves on each side

261   along the trunk. A dorsal vertebral groove runs between the head and the base of the tail. The

262   tail is one-half or slightly longer than one-half of total length. The tail has a cylindrical base, but

263   becomes bilaterally compressed posteriorly, with evident dorsal and ventral fin folds extending

264   distally. The end of the tail displays a rounded outline in lateral view (Fei & Ye, 2001). Toes in

265   the hind limb are reduced to four (Fei et al., 2006; Fei & Ye, 2001), although occasional

266   developmental anomalies are found in some individuals (see below). Terminal digits are claw-

267   like, covered with a black cornified epidermal sheath.

268

Dermal skull roof

270 The skull roof is flat, longer than wide as in other congeneric species (Fei et al., 2006). The

271 snout follows the contour of the maxillary arc: most specimens display a squarish outline, in

272 contrast to the rounded snout in other congeneric species (e.g., *Batrachuperus pinchonii*, *B*.

273 *karlschmidti*, *B. tibetanus*). The maximum width of the snout across the anterior borders of

274 orbits is much narrower than the maximum width of the skull at the cranio-mandibular joints,

275 thus giving a more or less trapezoidal outline of the skull roof in dorsal view (Fig. 2; Video S1).

276 This outline differs from that in *B. pinchonii*, which has a more rounded snout than *B*.

277 *londongensis*, and displays significant differences in the maximum width of the snout and at the

278 back of the skull (Fig. 2).

279 The paired premaxillae contact each other medially to close the anterior border of a large

280 anterodorsal fenestra (de Beer, 1937: cavum internasale) in the skull roof and an anteromedial

281 fenestra in the palate. The pars dentalis as the tooth-bearing part of the premaxilla forms the

282 anterior wall of the snout between the external nares, but its lateral extension articulates with the

283 maxilla to form the medial half of the ventral border of the narial opening. The anterior surface

284 of the premaxilla is penetrated by several small foramina. The pars dorsalis (alary process) of

285 the premaxilla ascends from the midlength of the pars dentalis, with the entire spine of the

286 process set in a groove on the anterodorsal surface of the nasal bone; therefore, the alary process

287 essentially contributes no part to the lateral border of the anterodorsal fenestra. A similar pattern

288 is seen in *B. tibetanus* (FMNH 5901), but not in other species of the genus.

289 The paired nasals are strongly widened to display a dimension almost twice the width of

290 the frontals, a plesiomorphic feature in urodeles as commonly seen in other hynobiids (Dunn,

291   1923; Gao & Shubin, 2012; Jia & Gao, 2016a). In dorsal view, the nasal is a large plate,

292   irregular in shape, meeting its counter element along a midline suture. The nasal has an anterior

293   process, which is medially notched for the large anterodorsal fenestra and laterally notched for

294   the narial opening. A lateral process of the nasal is in limited contact with the lacrimal, because

295   a large part of the latter bone overlaps the prefrontal (Fig. 2). The dorsal surface of the nasal is

296   smooth, but is penetrated by several tiny foramina (foramen mediale nasi of Francis, 1934) that

297   serve as passage of ultimate twigs of the mesial branch of the ophthalmicus profundus nerve (CN

298   V^1) as seen in *Salamandra* (Francis, 1934). The nasal posteriorly overlaps the frontal

299   extensively, and laterally meets with the lacrimal and prefrontal. In dorsal view, the suture

300   between the nasal and frontal is located at the level of the anterior borders of the orbits.

301   The paired frontals are strongly elongated posteriorly, with a straight or slightly sigmoid

302   sutural contact along the midline. The paired elements occupy much of the interorbital area of

303   the skull roof, but form only a small part of the medial border of the orbit, with a large part of the

304   border furnished by the parietal. The frontal articulates with the nasal anteriorly and with the

305   prefrontal anterolaterally. Immediately behind the posterior process of the prefrontal, the lateral

306   border of the frontal curves downward to articulate with the orbitosphenoid; however, this

307   contact is limited to only the anterior one-third of the orbitosphenoid, with the posterior two-

308   thirds of the latter in contact with the parietal (Figs. 3,4). This short contact between the two

309   elements is also seen in *B. karlschmidti*, whereas in all other congeneric species the prefrontal

310   contacts over one-half of the dorsal margin of the orbitosphenoid (Figs. 3,4). Posteriorly, the

311   frontal overlaps the parietal extensively, with a strongly elongate posterior process extending to

312   the level of the medial (otic) process of the pterygoid. This strong posterior extension of the

313   frontal differs significantly from all other congeneric species, in which the frontal is

314   proportionally shorter and terminates roughly at the midlevel of the orbit (e.g., FMNH 49380: *B*.

315   *karlschmidti*; FMNH 5901: *B. tibetanus*). Along the medial border of the orbit, the lateral

316   margin of the frontal curves downward to meet the orbitosphenoid and the anterolateral process

317   of the parietal.

318   The parietal is the largest element on the skull roof, but is extensively overlapped

319   anteriorly by the posterior extension of the frontal. The paired parietals meet at a straight or

320   slightly curved midline suture, and have parallel lateral borders forming most of the medial rim

321   of the orbit. The main part of the parietal table, however, is expanded bilaterally to form robust

322   lateral "boots" in articulation with the squamosals. The posterior part of the parietal table is

323   rugose dorsally, and posteriorly bears a bony ridge that curves anteriorly to house a deep fossa

324   (cervical epaxial fossa); both the bony ridge and fossa serve as insertion of the anterior epaxial

325   muscles (Carroll & Holmes 1980; Duellman & Trueb, 1986; Elwood & Cundall, 1994). Slightly

326   anterior to the lateral boot of the parietal, the lateral surface of the parietal is pierced by a tiny

327   foramen that serves as the passage of the trochlear nerve (CN IV; Gaupp, 1911) as clearly seen in

328   several specimens (e.g., CIB 65I0013/14380, 14381, 14504, 14507, 14509). This foramen has

329   been identified in all other congeneric species that we have examined (*B. karlschmidti*, *B*.

330   *taibaiensis*, *B. tibetanus*, *B. pinchonii*, *B. yenyuanensis*) in this study and has also been reported

331   in several other salamanders (e.g., Francis, 1934: *Salamandra*; Wake, 2001: *Dicamptodon*;

332   AmphibiaTree, 2008: *Ambystoma*).

333   In both dorsal and lateral views, the parietal table sends an elongate anterolateral process

334   pinched between the frontal and orbitosphenoid (Figs. 3,4). Anteriorly, the pointed end of this

335   process terminates slightly anterior to the midlevel of the orbitosphenoid. At the posterior border

336   of the orbit, the parietal develops a short triangular process, which is ventrally directed in contact

337   with a distinct pillar-like bone that in turn is ventrally in contact with the pterygoid. This small

338   pillar is identified as the perichondral ossification of the ascending process of the palatoquadrate,

339   and the presence of such a distinct bony element in *Batrachuperus londongensis* differs from all

340   other congeneric species but *B. karlschmidti* and *B. taibaiensis* (see below).

341   The prefrontal is a robust element, set at an oblique position in front of the large orbit.

342   The prefrontal meets the nasal and frontal medially; it underlies the lacrimal anteriorly and the

343   facial process of the maxilla laterally. The posterolateral margin of the prefrontal is curved to

344   form the anterodorsal rim of the orbit. The prefrontal has a well-developed posterior process that

345   extends far posterior to the nasal-frontal suture. A similar pattern is seen in *Batrachuperus*

346   *tibetanus*, but this process is much shorter in other congeneric species (*B. karlschmidti*, *B.*

347   *taibaiensis*, *B. pinchonii*, *B. yenyuanensis*). A prefrontal is normally present in most

348   salamanders, but is absent in proteids, sirenids, and some but not all plethodontids (Trueb, 1993;

349   Reilly & Altig, 1996; Rose, 2003).

350   The lacrimal is a narrow and slightly elongate plate, with its main part overlapping the

351   prefrontal. The lacrimal is essentially rectangular, similar to that in *B. tibetanus* and *B.*

352   *yenyuanensis*, but differing from that in other congeneric species, in which the lacrimal is

353   triangular with a pointed anterior end (*B. pinchonii* and *B. taibaiensis*) or more or less "L"-

354   shaped with a short process bending posteromedially (*B. karlschmidti*). In *B. londongensis*, the

355   lacrimal has a limited contact medially with the nasal, but is in an extensive sutural articulation

356   laterally with the facial process of the maxilla. The canal for the nasolacrimal duct (ductus

357   nasolacrimalis) opens as a foramen posteriorly on the dorsal surface of the lacrimal (Fig. 2A),

358   with the anterior foramen opening on the anteroventral side of the lacrimal. As a common

359   feature seen in most of *Batrachuperus* species, the lacrimal extends anteriorly over the border of

360   the external naris, but is posteriorly blocked by the prefrontal-maxillary contact from entering the

361   border of the orbit (Fig. 2). In other hynobiids, the lacrimal variably enters the naris only (e.g.,

362   *Salamandrella*), enters the orbit only (e.g., *Pachyhynobius*, *Paradactylodon*, some but not all

363   species in *Hynobius*), or enters both the naris and orbit (e.g., *Liua*, *Onychodactylus*,

364   *Pseudohynobius*, *Ranodon*, some species of *Hynobius*).

365   The maxilla is extremely short, but massively built, laterally covering the facial area of

366   the skull. The pars dorsalis of the maxilla is a robust process that widens between the narial

367   opening and the orbit. The process has an extensive sutural articulation with the lacrimal but a

368   limited contact with the prefrontal posterior to the lacrimal. The lateral wall of the maxilla is

369   slightly convex, and in some specimens (e.g., CIB 14485, 14509) is penetrated by a small

370   foramen anteriorly close to the narial rim. Ventral to the narial opening, the anteroventral

371   process of the maxilla articulates with the premaxilla to form one-half of the ventral border of the

372   naris. The posterior border of the pars dorsalis forms a part of the orbital rim, with the remaining

373   part furnished by the prefrontal. On the inner side of the pars dorsalis, a deep groove leads to a

374   small opening of the infraorbital canal, through which the superior alveolar branch of the

375   trigeminal nerve (CN V^2) and its associated blood vessels pass as in other salamanders (Francis,

376   1934). In both neotenic and postmetamorphic individuals, the short posteroventral process of the

377   maxilla terminates at a level far anterior to the midlevel of the orbit. The short maxillary tooth

378   row contains no more than 18 teeth. The tooth row terminates close to the posterior extremity of

379   the maxilla.

380   The septomaxilla is a small bone exposed anteromedial to the narial border of the

381   maxilla. A septomaxilla is present in all hynobiids, and is also present in some other groups of

382   urodeles (Rose, 2003: ambystomatids, dicamptodontids, rhyacotritonids, and some but not all

383   plethodontids). The absence of this element in several groups (sirenids, cryptobranchids,

384   amphiumids, and proteids) cannot be simply explained as a "paedomorphic loss" (contra

385   Duellman & Trueb, 1986), because the absent condition is also seen in metamorphosed

386   salamandrids (Francis, 1934; Rose, 2003), let alone that the element is present in the Jurassic

387   neotenic salamanders *Beiyanerpeton* and *Qinglongtriton* (Gao & Shubin, 2012; Jia & Gao,

388   2016b). In this study, all known specimens of *Batrachuperus londongensis* consistently display

389   the septomaxilla in both neotenic and postmetamorphic adults. Ontogenetically, the

390   septomaxilla is ossified immediately before or during metamorphosis in *Onychodactylus*

391   (Vassilieva, Poyarkov & Iizuka, 2013), *Ranodon* (Schmalhausen, 1968; Lebedkina, 2004),

392   *Salamandrella* (Schmalhausen, 1958; Lebedkina, 1964; Regel, 1970), and *Hynobius* (Vassilieva

393   et al., 2015).

394

395   **Suspensorium**

396   The squamosal is roughly T-shaped with its widened proximal end in articulation with the lateral

397   "boot" of the parietal and a transverse bar extending ventrolaterally over the quadrate (Fig. S1).

398   In dorsal view, the transverse bar is set at right angles in relation to the sagittal plane of the skull;

399   in occipital view, however, the transverse bar is set in an oblique position, sloping ventrolaterally

400   at a 45 degree angle towards the cranio-mandibular joint (Fig. S2). At the proximal end, a blunt

401   otic process projects anteriorly to articulate with the prootic, and a triangular process projects

402   posteriorly with its tip in contact with the opisthotic-occipital complex (Fig. 2). The squamosal

403   is slightly convex dorsally, but concave ventrally to embrace a large part of the quadrate.

404   The quadrate, as a principal element of the suspensorium, extends transversely beneath

405   the squamosal. In contrast to the squamosal, the quadrate has a widened lateral end and a medial

406   process extending towards the stapes (columella). In dorsal view, the lateral end of the quadrate

407   is exposed beyond the distal end of the squamosal, where the quadrate thickens ventrally to form

408   a cartilage-lined saddle in articulation with the articular in the mandible. From the distal end, a

409   short and flat process overlaps the posterolateral process of the pterygoid. As revealed in CT

410   images of several specimens (e.g., CIB 65I0013/14380, 14381, 14507), a tiny quadrate foramen

411   pierces the base of the pterygoid process as passage of a branch of the posterior condylar artery

412   and vein as generally seen in other tetrapods (Olson, 1966). A quadrate foramen has been

413   identified in the Early Cretaceous hynobiid-like salamander *Nuominerpeton* (Jia & Gao, 2016a),

414   whereas the occurrence of the foramen in extant hynobiids needs to be investigated thoroughly to

415   understand its phylogenetic significance. The ascending process of the quadrate extends beneath

416   the squamosal, and has a ligamentous connection with the stapes (see description of the stapes

417   below). Ossification of the quadrate occurs in all salamanders except sirenids (Rose, 2003).

418   Ontogenetic ossification of the quadrate in different hynobiid species can be variably before

419   (Suzuki, 1932; Lebedkina, 2004; Jia & Gao, 2016a), during (Lebedkina, 1964), or immediately

420   after metamorphosis (Vassilieva et al., 2015).

421   The pterygoid is triradiate in ventral view (Fig. 4; Fig. S3). The anterolateral (palatal)

422   process is elongated, extending to a point slightly anterior to the midlevel of the orbit; thus, the

423   ligamentous connection with the maxilla is extremely short. As a common pattern in other

424   salamanders, all hynobiids have a ligamentous connection between the maxilla and pterygoid,

425   with the exception of *Pachyhynobius*, in which a bony contact between the two elements is

426   established (Fei et al., 2006). In *B. londongensis*, the ventral surface of the anterolateral process

427   is smooth, but the dorsal surface is grooved to receive a slender rod of cartilage (processus

428   pterygoideus of the palatoquadrate), which extends along the entire length of the anterolateral

429   process of the pterygoid.

430   The posterolateral (quadrate) process of the pterygoid is slightly shorter than the

431   anterolateral process. A large part of the former process underlays the quadrate to reinforce the

432   cranio-mandibular joint. In addition to serving as a part of the suspensorium, the pterygoid also

433   serves as insertion of adductor muscles, including the pterygoideus head of the adductor

434   mandibulae internus (Carroll & Holmes, 1980). The medial (otic) process of the pterygoid is

435   short, but turns dorsally to meet a small pillar (ossified ascending process of the palatoquadrate);

436   thus, the process has no bony contact with the parasphenoid. Lack of a synostotic contact

437   between the pterygoid and parasphenoid is a common pattern in all other *Batrachuperus* species.

438   As mentioned above, it is of special interest to note the presence of a short pillar

439   upholding the parietal immediately anterior to the prootic (Figs. 2,3). To our knowledge, this

440   short pillar represents the perichondral ossification of the ascending process of the

441   palatoquadrate (Trueb, 1993: metapterygoid; Rose, 2003: epipterygoid). The short pillar is set in

442   a vertical or slightly oblique orientation, dorsally in articulation with a downward process of the

443   parietal and ventrally with the upward medial process of the pterygoid. In other salamanders, the

444   ascending process of the palatoquadrate normally remains unossified, whereas a "certain amount

445   of perichondral ossification" of the process has been documented in *Salamandra* (Francis, 1943:

446   26) as part of the suspensorium.

447   In this study, all of the adult specimens of *Batrachuperus londongensis* that we have

448   examined consistently show the presence of this pillar in the same position, and the same contact

449   patterns of the bone with the parietal and pterygoid can be seen in both dorsal and lateral views

450   (Figs. 2,3). CIB 14500 is a postmetamorphic juvenile, which shows that this pillar is not yet

451   ossified, as the individual also lacks ossification of the articular in the lower jaw (see below).

452   However, *B. karlschmidti* (FMNH 49380) and *B. taibaiensis* (CIB 20040235) are the two

453   congeneric species that show the presence of this bone and the same articulation patterns as in *B.*

454   *londongensis*. In other hynobiids, ossification of the pillar as part of the suspensorium is also

455   seen in *Paradactylodon mustersi* (FMNH 211936) and *Pseudohynobius flavomaculatus* (CIB

456   79I0107/17344). Whether this ossification represents a plesiomorphic feature with a

457   homologous origin or a derived state independently acquired needs to be investigated in a

458   phylogenetic analysis.

459

460   **Palate and braincase**

461   Formation of the palate involves the partes palatina of the premaxillae and maxillae, the vomers,

462   and the anterior portion of the parasphenoid. The partes palatina of the premaxillae are the

463   lingual shelves of the premaxillae that meet at the midline to close the anterior border of the

464   large palatal fenestra (Fig. 4; Fig. S3). The fenestra (Schmalhausen, 1968: intervomerine cleft;

465   Trueb, 1993: anteromedial fenestra) is the palatal opening for the intermaxillary gland

466   (Schmalhausen, 1968). Laterally, the pars palatina of the maxilla contacts the vomer to complete

467   the lateral rim of the palate.

468   In some neotenic individuals (e.g., CIB 14381, 14482), the ossified palatine is retained as

469   a discrete element either in articulation with or free from the anterior process of the pterygoid on

470   both sides of the palate (Figs. 2–4). In these specimens, the toothless palatine occurs as a small

471   plate or a slender bar. The palatine is entirely resorbed in all other hynobiids in the adult stage as

472   is commonly seen in other salamanders except sirenids (Worthington & Wake, 1971; Smirnov &

473   Vassilieva, 2002; Rose, 2003); therefore, the retention of this element as an ossification in some

474   but not all specimens in *Batrachuperus londongensis* can be interpreted as an ontogenetic

475   feature. This interpretation is supported by the hynobiid-like fossil salamander *Nuominerpeton*

476   *aquilonaris* of Early Cretaceous age from China, which displays normal resorption of the

477   palatine at metamorphosis (Jia & Gao, 2016a). Furthermore, none of the specimens of *B*.

478   *londongensis* that we examined have shown a separate palatine at a postmetamorphic stage, and

479   large neotenic individuals (e.g., CIB 65I0013/14380, 14484, 14485) also lack this element.

480   Because those specimens having a discrete palatine are apparently adult individuals, ontogenetic

481   resorption of the element in these individuals seems to be delayed until after sexual maturity.

482   The vomer is a large plate, irregular in shape, slightly longer than wide. The two vomers

483   are widely separated from one another, thus allowing the parasphenoid to enter the posterior

484   border of the anteromedial fenestra (Fig. 4; Fig. S3). This pattern is consistently observed in all

485   specimens, and thus is recognized in this study as a unique feature different from all other

486   species in *Batrachuperus* and other hynobiids as well. Jömann, Clemen & Greven (2005: fig.

487   33) figured *Ranodon sibiricus* at the adult stage as showing no midline contact of the vomers, but

488   this was probably based on juvenile or subadult specimens (Jömann, Clemen & Greven, 2005:

489   table 1: TL= <150 mm) as the nasals are widely separated (Jömann, Clemen & Greven, 2005:

490   fig. 32) in contrast to the condition in fully grown adults (maximum TL= 250 mm) as figured in

491   Fei et al. (2006: fig. 67). In *B. londongensis*, the medial border of the vomer is slightly concave,

492   forming the entire lateral margin of the anteromedial fenestra (Fig. 4; Fig. S3). Posterolaterally,

493   the vomerine plate is notched for the choana, with a small triangular process projecting towards

494   the orbit to embrace the notched choana. However, a retrochoanal (postchoanal) process is

495   absent, as a laterally directed process to block the posterior border of the choana is clearly

496   lacking. Another projection, medially attached to the parasphenoid, represents the posterior

497   process of the vomer (Fig. 4; Fig. S3).

498   A large part of the ventral surface of the vomer is smooth, except for a small tooth-

499   bearing area medial to the choana. The vomerine teeth are four to eight in number, arranged in a

500   linear fashion to form a straight row. The two vomerine tooth rows are widely separate but

501   slightly oblique, convergent anteriorly and divergent posteriorly. This arrangement differs from

502   most other congeneric species: in them the vomerine tooth row is more or less arched and

503   parallel to the maxillary tooth row. Close to the premaxilla-vomer suture, the vomer is

504   penetrated by two to three small foramina observed in several specimens (CIB 65I0013/14380,

505   14381, 14504, 14509; Fig. S4), probably for passage of the ramus ventralis of the trigeminal

506   nerve (CN V[1]) and the ramus palatinus of the facial nerve (CN VII) to supply the mucous

507   membranes of the mouth, as in other salamanders (Francis, 1934: *Salamandra salamandra*;

508   Cloete, 1961: *Rhyacotriton olympicus*).

509   The parasphenoid is a dermal bone that forms a large median plate, roughly rectangular

510   in outline, with straight lateral borders parallel to one another. The anterior process of the

511   parasphenoid contributes to part of the palate and closes the posterior border of the anteromedial

512   fenestra (Fig. 4; Fig. S3). The anterolateral part of the parasphenoid bears a flat facet, where part

513   of the vomer posterolateral to the anteromedial fenestra is attached. The lateral edge of the

514   parasphenoid curves dorsally, with a narrow groove in articulation with the ventral edge of the

515   orbitosphenoid. Posteriorly, the basal plate of the parasphenoid is widened to form the lateral ala

516   that floors the otic capsule. Close to the anterolateral border of the basal plate, a pair of internal

517   carotid foramina penetrates the parasphenoid as passage of the internal carotid arteries. As

518   observed in several specimens (CIB 65I0013/14380, 14381, 14482, 14504, 14507, 14509), more

519 than one foramen may occur on either side of the parasphenoid, possibly indicating minor

520 branches of the artery. The lateral ala has no bony contact with the otic process of the pterygoid,

521 but has an articulation with the prootic (Fig. 4; Fig. S3). The posterior end of the parasphenoid

522 forms a blunt posteromedian process, which furnishes the ventral rim of the foramen magnum.

523   The orbitosphenoid (sphenethmoid) as an endochondral bone is a rectangular plate that

524 covers a large part of the anterolateral wall of the braincase. The bony plate dorsally articulates

525 with the frontal and parietal, but in some specimens (e.g., CIB 65I0013/14380) it also articulates

526 with the prefrontal (Figs. 3,4; Fig. S1). The entire ventral edge of the orbitosphenoid meets the

527 parasphenoid. The anterior edge of the orbitosphenoid is vertical, forming a straight border of

528 the orbitonasal fenestra; the posterior border, however, is deeply notched for the optic foramen,

529 carrying the optic nerve and its associated vessels (Francis, 1934; Fox, 1959). There is no

530 foramen in the orbitosphenoid as passage of the oculomotor nerve (CN III); instead, this nerve

531 passes through the optic-oculomotor commissure, which is covered by cartilaginous tissues

532 posterior to the orbitosphenoid. This pattern of cranial nerves exiting through the anterolateral

533 wall of the braincase has been recognized as a diagnostic feature of the Hynobiidae (Jia & Gao,

534 2016a), differing from the sister group Cryptobranchidae, in which the optic foramen is fully

535 surrounded by the bony rim of the orbitosphenoid.

536   A separate operculum is absent in *B. londongensis*, as is common in most of other

537 hynobiids but *Hynobius*, in which the operculum is present as a separate element (Monath, 1965;

538 Rose, 2003). An operculum is figured as present in *Liua shihi* (Zhang, 1985) and *Ranodon*

539 *sibiricus* (Jömann, Clemen, & Greven, 2005: fig. 34); however, the element that is labeled in

540 both cases seems to be the stapes as it has a rounded footplate fused with the stylus.

541   No operculum, bony or cartilaginous, is identified in any of the specimens. The stapes

542   (columella) has a massive and disc-like footplate covering the foramen ovalis. The stylus is

543   extremely short, fused with the footplate proximally but with a small facet at its obtuse distal

544   end, where the ligamentum squamoso-columellare attaches; the ligament connects the stapes

545   with the quadrate and squamosal (Kingsbury & Reed, 1909). A stapedial foramen is

546   unexpectedly present on both sides in two specimens (CIB 65I0013/14380, 14381; both neotenic

547   individuals), penetrating the stylus horizontally (Fig. S2). In two other specimens (CIB 14507,

548   14509; both postmetamorphic individuals), a foramen penetrates left and right stapes, as well.

549   However, none of the other specimens, neotenic or postmetamorphic, show the presence of the

550   foramen. Therefore, the stapedial artery and/or the hyomandibular trunk of the facial nerve (CN

551   VII) in this species can variably pass through the stapedial foramen or below the short stylus. A

552   similar condition is known for *Ranodon sibiricus*: Schmalhausen (1968) described both present

553   and absent conditions of the stapedial foramen in specimens observed by him. Although Trueb

554   & Cloutier (1991) interpreted the absence of a stapedial foramen as a batrachian synapomorphy,

555   its presence in some salamanders is more likely to be a plesiomorphic feature for Urodela

556   because it also occurs in the stem caudate *Karaurus* (Ivachnenko, 1978; Estes, 1981).

557   Furthermore, the foramen is found in the Late Jurassic salamandroids *Beiyanerpeton* and

558   *Qinglongtriton* from China (Jia & Gao, 2016b). The discovery of the presence of this foramen in

559   some but not all postmetamorphic individuals in *Batrachuperus londongensis* casts more doubt

560   on our understanding of the evolution of this character.

561   The prootic is irregular in shape, covering the lateral wall of the anterior portion of the

562   otic capsule. The element dorsally articulates with the parietal, but a small part of its dorsal rim

563   underlays the squamosal as well. Ventrally, the prootic articulates with the lateral ala of the

564   parasphenoid. In lateral view, the alary process (optic process) of the prootic is a small flap

565   directed anterodorsally; the inferior process (basal process) of the prootic is more or less

566   triangular, with its ventral edge in articulation with the parasphenoid (Fig. 3; Fig. S1). A large

567   foramen faciale penetrates the lateral surface of the prootic as passage of the facial nerve (CN

568   VII).

569   The opisthotic and exoccipital are fully fused to form an opisthotic-exoccipital complex

570   covering the posterior wall of the braincase. The complex dorsally articulates with the parietal

571   and ventrally with the parasphenoid; in dorsal view, it is swollen posterolaterally as the housing

572   of the auditory capsule. The opisthotic portion of the complex borders the fenestra ovalis

573   anteriorly, whereas its exoccipital part borders the foramen magnum posteromedially and bears

574   the occipital condyle posteriorly in articulation with the cotyle of the atlas (Fig. S2). At the base

575   of the occipital condyle, the complex in penetrated by the foramen post-oticum (Fig. S2) through

576   which the combined glossopharyngeus-vagus nerves passes (CN IX + X; Francis, 1934). In all

577   hynobiids the opisthotic-exoccipital complex is fused and the prootic free (Carroll & Holmes,

578   1980; contra Trueb, 1993: three separate elements), except for *Onychodactylus*, in which the

579   prootic is fused to the opisthotic-exoccipital complex (Smirnov & Vassilieva, 2002; Vassilieva,

580   Poyarkov & Iizuka, 2013). In occipital view, the foramen magnum is roughly triangular in

581   outline. The dorsal rim of the foramen has a median gap where the cartilaginous tectum

582   synoticum attaches below the parietals. The ventral border of the foramen magnum is largely

583   formed by the posteromedian process of the parasphenoid.

584

585   **Mandible**

586   As in all cryptobranchoids (hynobiids and cryptobranchids), the lower jaw of *Batrachuperus*

587   *londongensis* consists of the dentary, prearticular, angular, and articular. In addition, a small

588   posterior mental process seen in all specimens at the symphysis gives a clear indication of the co-

589   ossification of a mentomeckelian element with the dentary (Fig. 5; Fig. S3).

590   The dentary is the largest bone of the mandible, covering most of its lateral and ventral

591   aspect. The lateral surface of the dentary is smooth, slightly swollen along the lower border but

592   weakly concave along the tooth row. A large foramen is often located at a position slightly

593   posterior to the midlevel of the dentary tooth row (Fig. 5). This foramen marks the passageway

594   of the mandibularis externus nerve (CN V_3), innervating both the skin and the muscle (M.

595   intermandibularis) between the two rami of the lower jaw (Francis, 1934). Posteriorly, the

596   dentary terminates at a robust process below the cranio-mandibular joint.

597   Posteroventral to the dentary, the angular bone is exposed in medial, ventral, and lateral

598   views. As observed in both lateral and ventral views, the angular is slightly thickened

599   posteriorly but narrows anteriorly, where it is wedged between the prearticular and the dentary

600   (Fig. 5; Fig. S3). The pointed anterior process terminates at a level slightly posterior to the

601   anterior extremity of the anterolateral process of the pterygoid, and the thickened posterior end

602   forms the posteroventral extremity of the mandible. In medial view, a small angular foramen

603   opens anteroventrally at the angular-prearticular suture, close to the anterior end of the angular

604   and below the coronoid process of the prearticular.

605   The prearticular is a large element covering most of the medial aspect of the jaw.

606   Anteriorly, the bone terminates at a point close to the mandibular symphysis. Posterodorsally,

607   the prearticular rises to form a large ascending process (coronoid process) that serves as insertion

608   of the adductor mandibulae internus. The process slopes downward posteriorly and continues as

609   a ridge that attaches to the medial side of the articular at the glenoid fossa. Below and

610   posteroventral to the coronoid process, the prearticular is penetrated by one or two foramina

611   (inferior dental foramina) as passage of the inferior alveolar ramus of the facial nerve (CN VII)

612   and the alveolar artery (Francis, 1934). There is often a third foramen that serves as passage of

613   the same nerve and vessel opening more anteroventrally at the tip of the angular bone.

614   The articular is well ossified in adults as in other extant species and fossil relatives of

615   hynobiids but is absent in cryptobranchids (Reese, 1906; Rose, 2003; Jia & Gao, 2016a). In

616   comparison to the angular, the articular is slightly shorter but more stoutly built. In dorsal view,

617   the anterior process of the articular extends between the prearticular and dentary, terminating at

618   an obtuse tip medial to the coronoid process of the prearticular (Fig. 5). The slightly expanded

619   posterior part of the articular is in articulation with the quadrate. As revealed from CT-scanned

620   images, a tube-like canal runs horizontally through the articular as the passage of the ramus

621   hyomandibularis of the facial nerve (CN VII); whether this pattern occurs in other congeneric

622   species and other hynobiids needs to be thoroughly investigated. Ontogenetically, the articular

623   ossifies slightly later than the septomaxilla after metamorphosis (Smirnov & Vassilieva, 2002;

624   Rose, 2003; Lebedkina, 2004; Vassilieva, Poyarkov & Iizuka, 2013; Vassilieva et al., 2015);

625   thus, presence of a bony articular is a clear indication of maturity in fossil and extant hynobiids

626   (Jia & Gao, 2016a). In this study, CIB 14500 is a postmetamorphic juvenile (TL= 110 mm;

627   SPL= 60.24 mm), which displays a typical postmetamorphic pattern of the hyobranchium but

628   shows no ossification of the articular. Once again, comparison of this with other specimens

629   indicates that the articular is ossified after metamorphosis in *Batrachuperus londongensis*. This

630   ossification sequence of the articular is similar with some other hynobiids, for example,

631   *Onychodactylus japonicus* (Smirnov & Vassilieva, 2002) and *Hynobius formosanus* (Vassilieva

632 et al., 2015), but differs from that in *Ambystoma*, in which the element is ossified during

633 metamorphosis (Reilly, 1987).

634

Dentition

636 Tooth-bearing elements in *Batrachuperus londongensis* include the premaxilla, maxilla, vomer,

637 and dentary. The premaxilla carries seven to nine teeth; the tooth rows on both sides are slightly

638 curved to form a broad arc, corresponding to the blunt snout. The maxilla carries 16–18 teeth,

639 with the tooth row terminating at the posterior extremity of the maxilla.

640   As described above, each vomer bears a single tooth row containing four to eight teeth.

641 The tooth row is essentially straight, but arranged obliquely medial to the choana with the two

642 tooth rows slightly converging anteriorly. The tooth rows are set far apart from one another,

643 corresponding to the separation of the vomers. Other palatal elements, including the

644 parasphenoid and pterygoid, are entirely edentulous.

645   The dentary tooth row is slightly longer than that of the maxilla, terminating posteriorly

646 at a point slightly anterior to the coronoid process of the prearticular. There are 20–25 teeth on

647 the dentary. All marginal teeth and vomerine teeth are pedicellate, with the basal pedicel and

648 crown separated by a poorly mineralized dividing zone. Tooth crowns are bicuspid as

649 commonly seen in most salamanders.

650

Hyobranchial apparatus

652 The hyobranchial apparatus in *Batrachuperus londongensis* has been shown to have two

653 different patterns related to life-history differences (Fei et al., 2006: fig. 69). The neotenic

654   pattern retains some of the larval branchial arches, and thus displays more complex structures

655   than in the postmetamorphic pattern (Fig. 6; Fig. S3).

656   Cartilaginous elements cannot be observed in our CT-scanned images, but can be

657   detected in cleared and stained specimens (Fig. 6). A cornua is present as a partly mineralized

658   median plate in the postmetamorphic pattern, whereas it is absent in neotenes (Fig. 6A,B). In

659   both neotenic and postmetamorphic individuals, the paired radial loops stemming from

660   basibranchial I (anterior copula) extend anteriorly, then curve laterally in continuation with the

661   ceratohyal. Therefore, the paired radial loops do not cross one another, in contrast to

662   *Batrachuperus pinchonii* and some other hynobiids (*Onychodactylus*, *Hynobius*,

663   *Pseudohynobius*, *Pachyhynobius*), in which a figure 8-shaped pattern is formed by a complex

664   crossing of the radial loops (Larson et al., 1996; Rose, 2003; Xiong et al., 2013b).

665   Basibranchial I (anterior copula) remains cartilaginous in both neotenic and

666   postmetamorphic individuals as in all other hynobiids except *Onychodactylus*, in which the

667   element is partly ossified as a short stub (Fukuda, 1930; Smirnov & Vassilieva, 2002; Xiong et

668   al., 2013b). Presence or absence of basibranchial II (posterior copula, os thyroideum of Rose,

669   2003) was previously unknown for *Batrachuperus londongensis*. Observation of multiple

670   specimens in this study reveals that basibranchial II is well ossified, displaying two different

671   patterns that may reflect developmental differences (see below): most specimens have an

672   anteriorly directed rod jointed with a transverse bar to form a simple inverted "T"-shaped

673   structure (Fig. 6B; Fig. S3A–E); other specimens have a long anterior rod connected with a

674   complex base, which displays multiple short branches directed posteriorly, termed here the

675   "fork"-shaped pattern (Fig. S3F). None of the specimens on which this study is based shows an

676   anchor-shaped basibranchial II, a configuration that has been recognized as a plesiomorphic

677   condition for urodeles (Jia & Gao, 2016b). The anchor-shaped basibranchial II occurs in the

678   stem caudate *Karaurus* (Ivachnenko, 1978; Estes, 1981), basal cryptobranchoid *Chunerpeton*

679   (Gao & Shubin, 2003), and basal salamandroid *Beiyanerpeton* (Gao & Shubin, 2012). The

680   plesiomorphic pattern is not seen in any extant hynobiids (see Xiong et al., 2013b), but occurs in

681   the basal hynobiid *Nuominerpeton* (Jia & Gao, 2016a).

682   Hypobranchial I and ceratobranchial I remain separate in *Batrachuperus londongensis*, in

683   contrast to the fusion in *B. pinchonii*, *B. tibetanus* (Fei et al., 2006), and several other hynobiids

684   (*Ranodon*, *Hynobius*, *Pseudohynobius*, *Salamandrella*, *Liua*) (Fei et al., 2006; Zhang et al., 2009;

685   Xiong et al., 2013b). Hypobranchial I in most specimens remain cartilaginous, but ossification

686   of the element occurs in large neotenes (CIB 65I0013/14380, 14381). CIB 14504 is the only

687   postmetamorphic individual that has it as a bony rod (Fig. 6B; Fig. S3B). Ceratobranchial I is

688   increasingly ossified ontogenetically in neotenes (CIB 65I0013/14380, 14381, 14482, 14484,

689   14485, 14499), but it remains cartilaginous in all postmetamorphic individuals. Whether bony or

690   cartilaginous, the distal end of ceratobranchial I is slightly hooked, bearing a small process that

691   curves posterodorsally (Figs. 6,7; Video S1).

692   Hypobranchial II and ceratobranchial II are both ossified as separate elements as in all

693   other hynobiids (Fei et al., 2006; Xiong et al., 2013b). The former element is basically rod-like,

694   slightly thicker posteriorly than anteriorly; the shaft can be relatively straight or slight curved

695   laterally. Ceratobranchial II is much longer than hypobranchial II, and often displays an

696   expanded distal end, which is bilaterally compressed into a distal plate. This is especially the

697   case in large neotenes, including the holotype. At midlength in the long rod, a prominent process

698   projects dorsomedially where the subarcualis rectus II attaches as in *Amphiuma* (Erdman &

699   Cundall, 1984). Ceratobranchials III and IV are normally absent in postmetamorphic individuals

700 (but see below), whereas they are present as bony elements in neotenes (Figs. 6,7). CIB 14487 is

701 a postmetamorphic young adult (TL= 164 mm; SPL= 89.27 mm); its adulthood is indicated by

702 ossification of the articular in the lower jaw, but it displays remnant ceratobranchial III in the

703 process of being resorbed (Fig. S3E).

704   The ceratohyal in both postmetamorphic and neotenic individuals is distally ossified, with

705 large adults showing more extensive ossification than smaller ones. In the holotype (CIB

706 65I0013/14380), the largest specimen known for the species (TL= 265 mm) and a neotene, over

707 60% of the ceratohyal is ossified as a robust element, leaving only the anterior one-third

708 cartilaginous (Fig. 7B; Fig. S3A). The ossified part of element has a prominent ridge

709 posterodorsally bearing a ligamentous connection with the suspensorium (Trueb, 1993; Rose,

710 2003). Partial ossification of the ceratohyal is also seen in all other species of *Batrachuperus*: *B.*

711 *pinchonii* (Zhang et al., 2009: fig. 24); *B. tibetanus* (FMNH 5901); *B. yenyuanensis* (FMNH

712 49371); *B. karlschmidti* (FMNH 49380); *B. taibaiensis* (CIB 20040235). Among other

713 hynobiids, partial ossification of the ceratohyal distally occurs in *Pachyhynobius*

714 *shangchengensis*, *Liua shihi*, and *Ranodon sibiricus* (Zhang, 1985; Fei et al., 2006).

715

716 **Axial skeleton**

717 As consistently observed from all *B. londongensis* specimens studied here, the vertebral column

718 consists of 18 presacral vertebrae, including the atlas, plus a single sacral, three to four

719 caudosacrals, and 29–30 caudal vertebrae (Fig. 7; Video S2). The number of the presacral

720 vertebrae is different from the type species, *Batrachuperus pinchonii* (Zhang et al., 2009; Xiong

721 et al., 2013a; but see Litvinchuk & Borkin, 2003: 16–17), as well as several other congeneric

722 species (*B. tibetanus*, *B. karlschmidti*, and *B. yenyuanensis*), which have 17 presacrals by our

723   own observation. Among other hynobiid species, the number of presacral vertebrae ranges from

724   15 in *Ranodon sibiricus* to 22 in *Onychodactylus fischeri* (Litvinchuk & Borkin, 2003).

725   In both dorsal and ventral views, the atlas is widened anteriorly, where it bears a pair of

726   cotyles that receive the occipital condyles. Anteroventral to the cotyles is the odontoid process

727   (tuberculum interglenoideum), which bilaterally articulates with the exoccipitals at the rim of the

728   foramen magnum. Posterior to the odontoid process, the ventral surface of the atlas is penetrated

729   by a pair of foramina through which the first pair of spinal nerves pass. The atlas has no

730   transverse process or free ribs.

731   In all trunk vertebrae, the centrum is more or less cylindrical and is deeply amphicoelous.

732   There is no significant change in length of the centrum along the trunk series, and all trunk

733   vertebrae bilaterally bear transverse processes that are directed posterolaterally. A shallow

734   groove is visible on the posterior surface of the transverse process, indicative of fusion of the

735   dorsal diapophysis with the ventral parapophysis. Because of this fusion, the articulation facets

736   of the diapophysis and parapophysis are confluent to receive the unicapitate ribs.

737   All presacral vertebrae except the atlas articulate with free ribs. The ribs associated with

738   the first three trunk vertebrae are more robust than the remaining ribs, having the distal end

739   expanded where the M. thoracic-scapularis attaches (Francis, 1934). In addition, the first pair of

740   ribs often bears a short uncinate process distally, so that the ribs are distally forked (e.g., CIB

741   14482, 14484, 14485, 14487; Fig. S3; Video S2). The ribs are similar in length for most of the

742   trunk series, but the posterior four to five pairs are abruptly shortened, with the last pair being a

743   remnant stub that is even shorter than the transverse process of the associated vertebra. All trunk

744   ribs are essentially single headed, although a shallow groove can be recognized posteriorly on

745   the rib head as indication of fusion of the dorsal tuberculum with the ventral capitulum.

746 Possession of unicapitate ribs is a diagnostic feature of the suborder Cryptobranchoidea (Dunn,

747 1923; Duellman & Trueb, 1986; Gao & Shubin, 2012; Jia & Gao, 2016a).

748 The single sacral vertebra is roughly the same size as the presacrals, but the transverse

749 process of the sacral is obviously more robust than that of the trunk vertebrae. The sacral rib is

750 elongated to at least twice the length of the transverse process, and curves ventrally to bear a

751 ligamentous connection with the ilium.

752 The three rib-bearing vertebrae following the sacral are identified as caudosacrals, with

753 the first haemal arch bearer marking the position of the anus. CIB 14485 is the only examined

754 specimen that displays four caudosacrals. These caudosacrals are roughly the same size as the

755 sacral vertebra, but ribs associated with them are greatly reduced, being slightly shorter than the

756 corresponding transverse process. Possession of three or more caudosacrals seems to be

757 plesiomorphic in urodeles (Gao & Shubin, 2001, 2012; Jia & Gao, 2016b). In fully grown

758 adults, 28–30 vertebrae follow the caudosacral series (Fig. 7; Video S2). The caudal vertebrae

759 normally have no free ribs, but occasionally remnant ribs occur in the first caudal in some

760 specimens (CIB 14484, 14487). All caudal vertebrae, except the posterior-most two or three,

761 ventrally bear a haemal arch, through which the haemal vessels pass.

762

763 **Appendicular skeleton**

764 ***Pectoral girdle and forelimbs***

765 A large part of the pectoral girdle remains cartilaginous, with only the scapulocoracoid co-

766 ossified as a single unit. A co-ossified scapulocoracoid occurs in all other salamanders but

767 sirenids, in which the scapula and coracoid remain separate (Noble, 1931). The scapulocoracoid

768 in *Batrachuperus londongensis* has an extremely short scapular blade as in other species of the

769   genus, but the dorsal border of the blade bears a distinct process projecting posterodorsally (Fig.

770   8; Video S2), a feature not seen in other *Batrachuperus* species. Because this process is

771   consistently prominent in all specimens under study (Table 1), it is recognized here as a

772   diagnostic feature of the species. Judging from its posterodorsal position, it unlikely served as

773   insertion of the opercular muscle, but more likely as ligamentous insertion of a levator muscle of

774   the shoulder; whereas it is the levator scapulae inferior or the intertransversaricus capitis inferior

775   needs to be further investigated (see Gaupp, 1898; Kingsbury & Reed, 1909; Goodrich, 1930;

776   Monath, 1965). Anterior to this process, the dorsal border of the scapular blade displays an

777   elliptical depression that articulates the suprascapular cartilage.

778   In the ventral part of the pectoral girdle, the procoracoid and coracoid are fully co-

779   ossified to form a large plate, which is expanded anteroposteriorly and curved ventromedially.

780   In lateral view, the anterior border of the coracoid plate is straight, but the ventral border is

781   rounded. Both the anterior and ventral borders are grooved to receive the cartilaginous part of

782   the procoracoid and coracoid, respectively. Close to the posterodorsal border of the coracoid

783   plate is a large glenoid fossa, which receives the head of the humerus. The glenoid fossa is

784   roughly circular, but its anteroventral rim is deeply notched where the crista ventralis of the

785   humerus fits (see below). Anteroventral to the glenoid fossa, a small supracoracoid foramen

786   (occasionally two openings) penetrates the coracoid plate as passage of the supracoracoideus

787   nerve (from the second and third spinal nerves) and its associated vessels (Francis, 1934). In

788   addition, it is interesting to note that some specimens (e.g., CIB 65I0013/14380, 14504) display

789   partial ossification of what otherwise is the cartilaginous part of the procoracoid and coracoid

790   (Fig. 8; Video S2). Because extra ossification of these cartilaginous parts occurs only in very

791   large specimens of both postmetamorphic and neotenic individuals, it can be viewed as a

792   developmental feature but one that cannot be tied with neoteny or metamorphosis.

793   The humerus is significantly longer than the ulna or radius. Proximally on its extensor

794   aspect, the crista dorsalis (dorsal crest) bears a prominent triangular or even knob-like projection,

795   onto which the M. subscapularis inserts (Francis, 1934). Proximally on the flexor aspect, the

796   crista ventralis (ventral crest) is a large triangular process, projecting anteroventrally where the

797   M. pectoralis and M. supra-coracoideus attach (Francis, 1934); the ventral crest merges with the

798   head of the humerus (or a facet in some specimens; see below). When the forelimb swings

799   forward, the crista ventralis fits into the notch of the anteroventral rim of the glenoid fossa as

800   mentioned above. Immediately ventral to the humeral head, a small but deep ventral depression

801   marks the insertion of the flexor muscle M. humero-artibrachialis (Francis, 1934). In young

802   adult specimens (e.g., CIB 14484, 14485, 14487), the humerus head is a cartilaginous cap, and

803   thus, CT-scanned images show a shallow facet; in fully grown adults (e.g., CIB 65I0013/14380,

804   14381, 14482, 14504, 14509), the humeral head is ossified into a large spherical condyle (Figs.

805   7, 8G–L). Among the latter, no postmetamorphic specimens show a cartilaginous cap, whereas

806   only relatively small neotenic individuals show a cartilaginous condyle. Distally, the olecranon

807   fossa on the extensor side of the humerus is extremely shallow, barely recognizable, but the fossa

808   cubitalis ventralis on the flexor side is a deep triangular depression, which receives the radius

809   when the forearm is flexed. In relatively small neotenes, the radial and ulnar condyles are

810   unossified, with the distal end of the humerus bearing two facets, where the cartilaginous ulnar

811   and radial condyles attach.

812   In the forearm, both the ulna and radius are straight, subequal in length and

813   approximately two-thirds the length of the humerus. The proximal end of the ulna is more

814   expanded than its distal end, and conversely the radius is a more expanded distally.

815   Posterolaterally, the ulna bears a bony crest that serves as insertion of the extensor of the forearm

816   (M. extensor antibrachii ulnaris). The radius is distally in articulation with the radiale and

817   intermedium. Close to its proximal end, the radius posterodorsally bears a prominent process,

818   which serves as ligamentous insertion of the M. humero-antibrachialis, the main flexor muscle of

819   the elbow (Francis, 1934). As described above for the humerus, in those specimens having a

820   well-ossified humeral condyle, the epiphyses of the radius and ulna are also ossified, leaving no

821   space for a cartilaginous cap.

822   Maximum ossification of the mesopodium in the forelimb displays a total of seven

823   elements as observed in several specimens including the holotype (CIB 65I0013/14380, 14381,

824   14482, 14505, 14507, 14509), whereas other specimens (CIB 14484, 14485, 14487) have six

825   ossified elements, with preaxial elements (radiale + element y) remaining cartilaginous (Fig.

826   9B,C). In those specimens showing maximum ossification, the intermedium proximally wedges

827   between the ulna and radius, and distally wedges between the centrale and ulnare (Fig. 9A,B,D).

828   The large radiale may represent a fusion of the radiale with element y, because no space for a

829   possible element y is present in these specimens. The single large centrale is in direct contact

830   with the radius, thus separating the radiale from contact with the intermedium. This pattern is

831   also seen in all other congeneric species, including *Batrachuperus yenyuanensis* (FMNH 49371),

832   which is the only known species of the genus in which two centralia occur. In *B. londongensis*,

833   the radiale is slightly smaller than the centrale, and articulates with the radius proximally, the

834   basale commune distally, and the centrale laterally. The basale commune is a large element,

835   roughly triangular in shape. It is in articulation with the centrale proximally and with metacarpal

836   1 and 2 distally. Distal carpal 3 is slightly smaller than distal carpal 4, and the two elements

837   articulate with metacarpal III and IV, respectively.

838   There are four digits in the manus, the pattern seen in most salamanders. Digit 3 is the

839   longest, having an extra phalange in comparison to the other digits. The phalangeal formula is 2-

840   2-3-2, a generalized pattern for most salamanders (Shubin & Wake, 2003). The terminal phalanx

841   of each digit is covered with a cornified sheath, possibly an adaptive feature correlated to living

842   in a mountain stream environment.

843

844   ***Pelvic girdle and hind limbs***

845   The pelvis in *Batrachuperus londongensis* displays the usual pattern that occurs in most other

846   salamanders: the paired ilia and ischia are ossified, whereas the pubis remains cartilaginous (but

847   see below). In addition, the ypsiloid cartilage is present as in some but not all salamanders (see

848   Hecht & Edwards, 1976, 1977). The ilium is roughly club-shaped, with a slightly thickened and

849   expanded ventral plate and a narrow dorsal blade. The ventral plate contributes to a large part of

850   the acetabulum and is ventrally in articulation with the ischium. The iliac blade is connected

851   with the sacral rib by a ligament. The bone is set in a more or less vertical position, whereas the

852   iliac blade is slightly inclined posteriorly.

853   The ischium is a large bony plate that is the main ventral element in the pelvis. The two

854   ischial plates meet ventrally to form a symphysal hinge articulation along the midline. In ventral

855   view, the ischium is anteriorly widened with a rounded border, to which the cartilaginous pubis

856   is attached (but see below), but projects laterally at the posteroventral border of the acetabulum.

857   Immediately posterior to the acetabulum, the lateral border of the plate is deeply notched

858   between the acetabulum and a large posterolateral process (ischial spine). The latter process

859   serves as origin of the flexor of the tail, M. ischio-caudalis (Francis, 1934). The elongate ischial

860   spine is significantly different from that in the type species *B. pinchonii*, in which the spine is

861   rudimentary (see Zhang et al., 2009).

862   The pubis often remains cartilaginous, as observed in several specimens (CIB 14482,

863   14484, 14485, 14487, 14507); however, in other specimens (CIB 65I0013/14380, 14381, 14504,

864   14509), the pubis is partly ossified, evidenced by the presence of a robust process anteroventral

865   to the acetabulum (Fig. 10A–D; Fig. S5). This interpretation is supported by the presence of an

866   obturator foramen at the base of the process, which marks the border between the pubis and

867   ischium (Fig. 10B). In addition, two of these specimens (CIB 14381, 14509) show that the

868   fusion of the ossified part of pubis to the ischium is not yet completed; thus, in these two

869   specimens the obturator foramen is still partly open anteromedially (Fig. 10D). In them, the

870   large ventral plate in the pelvis actually represents the ossification of the ischium and at least a

871   part of the pubis, and can best be termed a pubio-ischium.

872   It is also interesting to note that many specimens including the holotype display a second

873   pair of small foramina more posteriorly located at the base of the ischial spine (Fig. 10B,D,F,H).

874   To our knowledge, there are no publications that figured or described this pair of foramina, but

875   they are indeed present in both neotenic and postmetamorphic individuals of *Batrachuperus*

876   *londongensis*.

877   A Y-shaped cartilage (ypsiloid) is not shown in CT-scanned images, but is observed in

878   cleared and stained specimens (Fig. S5). This cartilage has been shown to be correlated with the

879   hydro-static function of the lungs (Whipple, 1906); that is, the salamander can easily raise its

880   head in the water by elevating the ypsiloid cartilage, thereby compressing the lower abdomen

881   and forcing the air in the lungs forwards to the anterior end; conversely, the salamander is able to

882   depress its head by lowering the ypsiloid cartilage, returning the air to the posterior portion of the

883   lungs, enabling the animal to swim to deeper water. The ypsiloid cartilage is present in

884   Hynobiidae, Cryptobranchidae, Salamandridae, and Ambystomatidae, but absent in Proteidae,

885   Plethodontidae, Sirenidae, and Amphiumidae (Hecht & Edwards, 1976, 1977).

886   The femur is a robust element roughly the same length as the humerus. As seen in the

887   holotype and several other specimens (CIB 65I0013/14380, 14381, 14504, 14507, 14509), the

888   strongly expanded proximal end bears a large bony condyle in articulation with the acetabulum

889   (Fig. 10I–L). In four other specimens (CIB 14482, 14484, 14485, 14487), however, the femur is

890   capped with cartilage; thus, CT images of these specimens display a gap between the femur and

891   acetabulum. On the extensor side, the femur bears a longitudinal ridge, extending from the

892   proximal end to the fibular condyle; this ridge serves as insertion of the M. pubo-ischio-

893   femoralis internus, a powerful extensor of the thigh (Francis, 1934). Posterior to this ridge and

894   close to the proximal end, a small tubercle marks the external trochanter (Fig. 10I,O), onto which

895   the M. caudalis-femoralis inserts (Francis, 1934). On the flexor side, the robust femoral

896   trochanter projects ventromedially as a twig-like process (Fig. 10I–P), onto which the M. pubo-

897   ischio-femoralis externus attaches (Ashley-Ross, 1992). The trochanteric crest extends from the

898   femoral trochanter distally along the shaft to the tibial condyle. On the distal end, both the tibial

899   and fibular condyles are well ossified to display a bony articulation with their corresponding

900   elements. The tibial condyle is much larger than the fibular condyle. As described above for the

901   proximal head, in some specimens (CIB 14482, 14484, 14485, 14487) the tibial and fibular

902   condyles are poorly ossified, with slightly concave depressions as indicative of a cartilage-

903   capped epiphysis.

904   The tibia and fibula are similar in length, but the former element is the more robust (Fig.

905   11). Proximally on its extensor aspect, the tibia bears a weakly developed tibial crest that serves

906   as a tendinous insertion of the M. extensor ilio-tibialis (Francis, 1934). Along the distal half of

907   the tibia is a well-defined bony ridge facing the fibula; this medial ridge probably serves as

908   insertion of the M. extensor cruris tibialis (Ashley-Ross, 1992). At the proximal end of the

909   medial ridge, a small but twig-like process provides a tendinous insertion of the M. pubo-ischio-

910   tibialis (Francis, 1934). The lateral side of the fibula is straight but the medial side concave, with

911   its distal end expanded medially to articulate with the tibia.

912   Maximum ossification of the mesopodium includes as many as nine tarsal elements (Fig.

913   11). As observed in several specimens (CIB 65I0013/14380, 14381, 14485, 14509), the

914   intermedium is a large element with its proximal process wedged between the tibia and fibula;

915   the intermedium distally articulates with a single centrale. The fibulare is roughly the same size

916   as the intermedium and is medially in extensive articulation with the latter. The tibiale is much

917   smaller than the fibulare, but medially articulates with the centrale. Among distal elements,

918   element y is more or less rounded, in articulation with the tibiale proximally, and with a large

919   basale commune laterally. Distal tarsal 3 and 4 are similar in size and both are in contact with

920   the centrale. Distal tarsal 5 is missing, what is likely related to the loss of digit 5. Distolaterally,

921   the postminimus is a small bone in contact with both the fibulare and metacarpal IV. According

922   to Shubin & Wake (2003), a postminimus is present in *Batrachuperus* and several other

923   hynobiids (*Liua*, *Ranodon*, *Salamandrella*, *Paradactylodon*), and also in the cryptobranchid

924   *Andrias*.

925   Several other specimens show less extensive ossification in the mesopodium than those

926   described above. As observed in four specimens (CIB 14482, 14482, 14484, 14487), all those

927   elements ossified already show essentially the same arrangement pattern as described above, but

928   have one or two of the preaxial elements (tibiale and element y) still unossified. In addition, in

929   none of these specimens is the postminimus ossified. Comparison of these specimens with those

930   described above indicates that element y ossifies before the tibiale, whereas the postminimus is

931   ossified after the tibiale; thus, the postminimus is the last tarsal element to be ossified

932   ontogenetically.

933   As in all congeneric species, *Batrachuperus londongensis* displays a reduction of hind

934   limb digits from five to four, with digit 5 missing. The phalangeal formula is 2-2-3-2, except for

935   two specimens (CIB 14484, 14504) that show developmental abnormalities (see below). The

936   terminal phalanges are covered with a cornified sheath as occurs commonly in other mountain

937   stream salamanders, including the Middle Eastern stream salamander *Paradactylodon* (Kami,

938   1999).

939   As mentioned above, two specimens (CIB 14484, 14504) show developmental

940   abnormalities in the hind limb. In CIB 14484, the right foot has four digits, but five in the left.

941   In keeping with the presence of digit 5, a distal tarsal 5 is also present in the left foot but not in

942   the right. The digital formula in this specimen is 2-2-2-2-2 in the right foot, and 2-2-3-2 in the

943   left. The other specimen (CIB 14504) has only three digits in left foot, with digit 1 entirely

944   missing; but there are four digits in the right. The left foot has only six tarsal elements, whereas

945   the right has ten, including two centralia. The six tarsals in the left may reflect abnormal fusion

946   of several bones: possibly fusion of the intermedium with the centrale, and fusion of distal tarsals

947   2+3. The fibulare is enlarged and roughly the same size as the intermedium. Both left and right

948   limbs have a small postminimus, indicative of this individual being a fully grown adult. The

949   digital formula of this specimen is ?-2-3-2 for the left foot, and is 2-2-2-2 for the right.

950

Discussion

952 The Longdong Stream Salamander, *Batrachuperus londongensis*, is a rare hynobiid species that

953 is of special interest because of a life-history that features facultative neoteny. In addition,

954 undertaking an osteological study of this salamander is urgent, because of its rarity and current

955 vulnerability to extinction (Jiang et al., 2016). From comparison with other species of the genus

956 and other hynobiids, our study has revealed several osteological features that are diagnostic of *B.*

957 *londongensis*, while several other features are shown to be of developmental, ecological, or

958 phylogenetic significance. We provide a discussion of these results below.

959

Osteological characterization of *Batrachuperus londongensis*

961 Previously, *Batrachuperus londongensis* had been diagnosed with reference only to external

962 morphological characters and the number of chromosomes (Liu & Tian, 1978; Fei, Ye & Tian,

963 1983; Fei et al., 2006). In supplementing the diagnosis of this species by inclusion of

964 osteological features, our study shows that some of these diagnostic features are also

965 phylogenetically significant in respect to both hynobiids and to the evolution of salamanders

966 more generally. Osteologically, *B. londongensis* shares with its congeneric species the following

967 derived characters: the maxilla is extremely short, posteriorly terminating at a level anterior to

968 midlevel of the orbit; the lacrimal extends anteriorly over the border of the external naris, but not

969 over the orbital border posteriorly (except for *B. taibaiensis*); a nasal-maxillary contact is absent

970 because the two elements are separated by the lacrimal; the otic process of the pterygoid has no

971 bony contact with the parasphenoid (except for *B. yenyuanensis*); the ceratohyal is distally

972 ossified; a single centrale (except for *B. yenyuanensis*) in the manus is in direct contact with the

973   radius, preventing the radiale from contacting the intermedium; the number of digits is reduced

974   from five to four in the pes (shared with *Salamandrella* and *Paradactylodon* as homoplasies);

975   terminal phalanges are covered with a cornified sheath (shared with *Onychodactylus*, *Liua*,

976   *Paradactylodon* as ecological homoplasies).

977   *Batrachuperus londongensis* is distinguished from *B. pinchonii* and all other congeneric

978   species by a combination of the following characters: alary process of premaxilla barely

979   contributing to border of anterodorsal fenestra (shared with *B. tibetanus*); suture between nasal

980   and frontal located at the level of anterior border of orbit; vomers do not contact at the midline

981   (unique); vomerine teeth four to eight in number, arranged in a straight line that is nearly

982   vertically oriented; the ascending process of the palatoquadrate is ossified as a pillar between the

983   parietal and the otic process of the pterygoid (shared with *B. tibetanus* and *B. taibaiensis*); radial

984   loops stemming from basibranchial I do not cross one another (shared with *B. pinchonii*, *B.*

985   *tibetanus*; unknown for other species); cartilaginous hypobranchial I and ceratobranchial I

986   remain separate (fused in *B. pinchonii* and *B. tibetanus*); presacral vertebrae 18 in number; the

987   scapular blade is extremely short, with a prominent posterodorsal process (unique); the ischial

988   plate is penetrated by a small nerve foramen, and the ischial spine is clearly more elongated than

989   in other species.

990

991   **Developmental features related to life-history differences**

992   As stated above (see Introduction), *Batrachuperus londongensis* may represent the only living

993   hynobiid that is facultatively neotenic, as both biphasic individuals and neotenes ("permanent

994   larval producers" of Rose, 2003) are known for the species. Based on our study of both neotenic

995   postmetamorphic specimens, we provide a discussion of life-history differences of the species as

996   presented below.

997   In terms of body size, neotenes tend to be larger than postmetamorphic individuals. The

998   holotype CIB 65I0013/14380 (TL= 265 mm) is the largest individual known for the species, but

999   still retains gill slits and a larval configuration of the hyobranchium (Fei et al., 2006). Because

1000   many relatively small specimens (TL= 162–241 mm) have completed metamorphosis, the

1001   presence of external gill slits and retention of a larval hyobranchium in large individuals cannot

1002   be logically interpreted as ontogenetic features always leading to metamorphosis in

1003   *Batrachuperus londongensis*. By contrast, the holotype and several other large individuals

1004   display fully ossified limbs and a postminimus in the pes, thereby giving a clear indication that

1005   these are fully grown adults, in spite of their retention of some larval features.

1006   The most striking morphological difference between neotenic and postmetamorphic

1007   individuals is seen in the hyobranchium. As figured in Fei et al. (2006: fig. 69f, g), neotenes

1008   always display a more complex hyobranchium than do postmetamorphic individuals, in which

1009   ceratobranchials III and IV are entirely missing. Among median elements, the inverted "T-

1010   shaped" basibranchial II occurs in both postmetamorphic and neotenic forms, whereas the

1011   "fork"-shaped pattern is seen only in some neotenes as a developmental feature. We provide a

1012   possible interpretation here: the "fork"-shaped pattern can be viewed as the initial larval pattern,

1013   with the posterior branches subsequently absorbed at metamorphosis, whereas in neotenes the

1014   absorption process is prolonged or delayed. This interpretation is supported by evidence that

1015   large neotenic individuals, including the holotype CIB 65I0013/14380, which display the

1016   inverted "T"-shaped pattern, still have a remnant of the posterior processes, whereas slightly

1017   smaller and presumably younger adults show the "fork"-shaped pattern.

1018   With respect to the laterally paired elements, both neotenic and postmetamorphic

1019 individuals show incomplete ossification of the ceratohyal, with large neotenes displaying more

1020 extensive ossification than smaller ones. This observation indicates that ossification of the

1021 ceratohyal terminates at metamorphosis, but continues in neotenes. Hypobranchial I is partly

1022 ossified in large neotenes, but the element is missing in typical postmetamorphic forms (see

1023 below). Ceratobranchial I is partly ossified only in neotenes. Evidently, ossification of the first

1024 branchial arch derivatives is terminated at metamorphosis, but is prolonged in neotenes.

1025 Ossification of hypobranchial II and ceratobranchial II is a common pattern in all hynobiids,

1026 whereas ceratobranchials III and IV are retained only in neotenic individuals, and are normally

1027 absent in postmetamorphic forms. CIB 14487 is a relatively small postmetamorphic adult, but it

1028 retains a remnant part of the ceratobranchial III bilaterally. Comparison of this specimen with

1029 those that show the typical postmetamorphic pattern of the hyobranchium indicates that

1030 resorption of larval arches can be prolonged until after metamorphosis is otherwise completed.

1031

1032 **Partial ossification of ceratohyal in hynobiids**

1033 Comparison of *Batrachuperus londongensis* with congeneric species and other hynobiids

1034 suggests that partial ossification of the ceratohyal is a feature of phylogenetic significance.

1035 Within *Batrachuperus*, a similar pattern of ossification of the ceratohyal occurs in *B. tibetanus*

1036 (FMNH 5901), *B. pinchonii* (Zhang et al., 2009: fig. 24), *B. karlschmidti* (FMNH 49380), *B.*

1037 *yenyuanensis* (FMNH 49371), and *B. taibaiensis* (CIB 20040235). Xiong et al. (2013b: fig. 1E

1038 and 1H) illustrated *B. pinchonii* and *Liua shihi* as having the ceratohyal entirely cartilaginous,

1039 but characterized this structure in the description as partly ossified in both species. Based on our

1040   own observations, we conclude that partial ossification of the ceratohyal occurs in all species of

1041   *Batrachuperus*.

1042   In other hynobiids, partial ossification of the ceratohyal occurs in the monotypic

1043   *Pachyhynobius shangchengensis* and in *Ranodon sibiricus* (Fei & Ye, 1983; Fei et al., 2006;

1044   however, Xiong et al., 2013b: fig. 1G shows no ossification in *R. sibiricus*), and in *Liua shihi*

1045   (Zhang, 1985; Fei et al., 2006; contra Xiong et al., 2013b: fig. 1, but mentioned as partly ossified

1046   in the description). In addition, our observation of a specimen of *Paradactylodon mustersi*

1047   (FMNH 211936) shows that it also displays a partly ossified ceratohyal. Another species,

1048   *Paradactylodon persicus* (MVZ 241494; AmphibiaTree, 2004) shows no ossification of the

1049   ceratohyal, but the specimen seems to be a young adult, as the nasals do not yet fully meet at the

1050   midline and a small parietal fontanelle is not yet completely closed. Ossification of the

1051   ceratohyal in four hynobiid genera (*Onychodactylus*, *Salamandrella*, *Pseudohynobius*, *Hynobius*)

1052   has yet to be recorded.

1053   In the closely related clade Cryptobranchidae, the distal end of the ceratohyal is ossified

1054   in the North American hellbender *Cryptobranchus alleganiensis* (Elwood & Cundall, 1994: fig.

1055   9; Rose, 2003: fig. 5), but not in the Chinese or Japanese giant salamander *Andrias* (Sato, 1943;

1056   Aoyama, 1930; Wu, 1982; Rose, 2003). Among non-cryptobranchoid salamanders, partial

1057   ossification of the ceratohyal is seen in some salamandrids (e.g., *Notophthalmus viridescens*) and

1058   some dicamptodontids (e.g., *Dicamptodon ensatus*), in *Siren* and *Pseudobranchus*, and in

1059   *Proteus* but not in *Necturus* (see Rose, 2003 for citations). Clearly, the distribution of this

1060   character needs to be scrutinized in a cladistic analysis to understand its phylogenetic

1061   significance.

1062

1063 **Ossification patterns of mesopodial elements and reduction of number of**

1064 **digits**

1065 Salamander limbs display variant structural patterns that provide significant information for

1066 addressing questions of morphological evolution in terms of ecological adaptation (Shubin &

1067 Wake, 2003). In this context, several limb features of *Batrachuperus londongensis*, including

1068 the arrangement of mesopodial elements and the reduction of the number of digits, are worth

1069 consideration in comparison with other congeneric species and other hynobiids as well.

1070 Patterns of limb structure in hynobiid salamanders have been documented for several

1071 genera (*Onychodactylus*, *Batrachuperus*, *Salamandrella*, *Liua*, *Ranodon*, *Paradactylodon*), but

1072 remain largely unknown or poorly known for several others (*Hynobius*, *Pachyhynobius*,

1073 *Pseudohynobius*). *Batrachuperus* has been regarded as having two centralia (Shubin & Wake,

1074 2003), but this interpretation was probably based on *B. yenyuanensis*, which indeed has two

1075 centralia; however, this study revealed that all other species of the genus, including the type

1076 species *B. pinchonii*, have a single centrale in both manus and pes. Although the single centrale

1077 is in direct contact with the radius in the forelimb, it does not contact the tibia in the hind limb.

1078 A direct contact of the centrale with the radius has been recognized as a peculiar feature in extant

1079 salamanders, as it also occurs in some lepospondyls and temnospondyls (Carroll, 1968; Carroll

1080 & Gaskill, 1978; Shubin & Wake, 2003). Regardless, *B. yenyuanensis* is the only species within

1081 *Batrachuperus* that possesses two centralia. Phylogenetic analysis based on molecular data has

1082 shown that *B. yenyuanensis* occupies a basal position in relation to other species of the genus

1083 (Chen et al., 2015); thus, the single centrale in these other species is likely to be a derived state

1084 acquired within *Batrachuperus*. Among other hynobiids, retention of two centralia is known for

1085   several taxa, including *Liua*, *Ranodon*, *Salamandrella*, and *Paradactylodon* (Shubin & Wake,

1086   2003).

1087   Comparison of specimens of *Batrachuperus* species reveals a delayed ossification of

1088   preaxial elements in both fore- and hind limbs. In the forelimb, fully grown adults of *B.*

1089   *londongensis* (e.g., holotype CIB 65I0013/14380, 14381, 14482, 14504) have a large radiale,

1090   which probably reflects fusion of the radiale with element y, whereas young adults (e.g., CIB

1091   14484, 14485, 14487) show no ossification of the radiale or element y. Whether the radiale and

1092   element y are co-ossified or fused together in fully grown adults needs to be verified by

1093   developmental evidence. In the hind limb, fully grown adults (e.g., CIB 65I0013/14380, 14381,

1094   14504, 14507, 14509) clearly show that the tibiale and element y are ossified as separate

1095   elements, with several young adults (e.g., CIB 14482, 14484, 14485) showing that element y is

1096   ossified before the tibiale. Comparisons with other species of *Batrachuperus* and other

1097   hynobiids are needed to understand the ontogenetic and phylogenetic significance of these

1098   patterns.

1099   According to Shubin & Wake (2003), a postminimus is present in *Batrachuperus*, several

1100   other genera of hynobiid salamanders (*Onychodactylus*, *Liua*, *Ranodon*, *Salamandrella*,

1101   *Paradactylodon*), and also the cryptobranchid genus *Andrias*. Comparison of specimens of

1102   congeneric species in this study leads us to concur with Shubin & Wake (2003) in that

1103   congeneric species in *Batrachuperus* indeed have a postminimus in pes, and this is probably the

1104   last limb element to be ossified ontogenetically, as the postminimus is observed in fully grown

1105   adults but not in those young adults that have element y, or element y and tibiale ossified (see

1106   above). The postminimus is absent in *Hynobius*, *Pachyhynobius*, and *Pseudohynobius* (Shubin

1107   & Wake, 2003). Although relevant information on presence/absence of this element is still

1108   sketchy for some hynobiid taxa, we interpret that possession of a postminimus as a

1109   plesiomorphic feature because it is widely distributed in the family Hynobiidae. However, how

1110   many taxa at generic level share the loss of the element as a homology, or independent loss of

1111   this element need to be scrutinized in a thorough phylogenetic analysis.

1112   Finally, *Batrachuperus londongensis* displays limb patterns commonly seen in other

1113   mountain stream salamanders: The number of digits is reduced from five to four in hind limb,

1114   and terminal phalanges in both fingers and toes are covered with a cornified sheath. These

1115   features have been recognized as corresponding to ecological adaptations of the salamanders to

1116   higher altitude mountain stream environments (Fei & Ye, 1984). These limb features are

1117   commonly seen in all other *Batrachuperus* species, and in other hynobiids (*Salamandrella*,

1118   *Paradactylodon*, and some species of *Hynobius*), which are also mountain stream dwellers

1119   (Reilly, 1983; Fei et al., 2006). Interestingly, there are some hynobiids (*Onychodactylus*,

1120   *Ranodon*, *Liua*) that are mountain stream dwellers, but none of these show reduction of digits

1121   from five to four in the pes; and *Onychodactylus* is the only genus other than those mentioned

1122   above has developed claw-like terminal phalanges with a cornified sheath (Fei et al., 2006).

1123

1124   **Conclusions**

1125   Our study of the osteological anatomy of *Batrachuperus londongensis* has led to the following

1126   conclusions:

1127   1) *Batrachuperus londongensis* is diagnosed by a set of osteological features, including

1128   unique features: alary process of premaxilla is excluded from the border of the anterodorsal

1129   fenestra; vomers lack medial contact; parasphenoid enters anteromedial fenestra; vomerine tooth

1130   row nearly vertical in position; presacral vertebrae 18 in number; scapular blade develops a

1131   distinct posterodorsal process.

1132   2) *B. londongensis* is among the few hynobiids that display perichondral ossification of

1133   the ascending process of the palatoquadrate as a part of the suspensorium.

1134   3) A stapedial foramen is unexpectedly present in some but not all specimens, an unusual

1135   feature that needs to be thoroughly investigated.

1136   4) Neotenic individuals display a more complex structural pattern of the hyobranchium

1137   than postmetamorphic individuals, most notably the retention of ceratobranchials III and IV.

1138   Neotenes also show increased ossification of hyobranchial elements during aging, in contrast to

1139   loss of elements by resorption in metamorphic individuals.

1140   5) *B. londongensis* has a single centrale in direct contact with the radius in the manus, but

1141   not with the corresponding element, the tibia, in the pes. In both fore- and hind limbs, delayed

1142   ossification of preaxial elements is a common pattern in both neotenes and postmetamorphic

1143   specimens.

1144   6) *B. londongensis* retains element y and the postminimus in the pes as a plesiomorphic

1145   pattern in hynobiids. Phylogenetic significance of the retention or loss of these limb elements

1146   within Hynobiidae requires a thorough investigation.

1147

Acknowledgements

1149   We thank Alan Resetar (Field Museum of Natural History) for access to comparative specimens

1150   under his care, and Zhe-Xi Luo (University of Chicago, Chicago, USA) for use of the CT

1151   scanner in his laboratory. Professor RC Fox (University of Alberta, Edmonton, Canada) read

1152   and commented on the manuscript, and Yu-long Li (Chengdu Institute of Biology, Chinese

1153   Academy of Sciences, Chengdu, China) helped with CT scanning of some specimens. We also

1154   thank Neil Shubin (University of Chicago) for discussion on ossification patterns and evolution

1155   of the mesopodium in salamanders. Two reviewers (M. Laurin and J. Ziermann) provided

1156   constructive comments and suggestions that lead to improvement of our manuscript.

1157

1158

1159   **REFERENCES**

1160   AmphibiaTree. 2004. *Batrachuperus persicus* (On-line), Digital Morphology. Accessed March

1161   14, 2017 at http://digimorph.org/specimens/*Batrachuperus_persicus*/.

1162   AmphibiaTree. 2008. "*Ambystoma gracile*" (On-line), Digital Morphology. Accessed April 5,

1163   2017 at http://digimorph.org/specimens/Ambystoma_gracile/head/.

1164   AmphibiaWeb. 2017. <http://amphibiaweb.org> University of California, Berkeley, CA, USA.

1165   (accessed 10 March 2017).

1166   Aoyama F.1930. Die Entwicklungsgeschichte des Kopfskelettes des *Cryptobranchus japonicus*.

1167   *Zeitschrift für Anatomie und Entwicklungsgeschichte* **93**:106–181.

1168   Ashley-Ross MA. 1992. The comparative myology of the thigh and crus in the salamanders

1169   *Ambystoma tigrinum* and *Dicamptodon tenebrosus*. *Journal of Morphology* **211**:147–163.

1170   DOI: 10.1002/jmor.1052110204.

1171   Boulenger GA. 1878. Description de deux genres nouveaux de la famille des salamandrides.

1172   *Bulletin de la Société Zoologique de France* **3**:71–71.

1173   Carroll RL. 1968. The postcranial skeleton of the Permian microsaur *Pantylus*. *Canadian*

1174   *Journal of Zoology* **46**:1175–1192.

1175   Carroll RL, Gaskill P. 1978. The order Microsauria. *Memoirs of the American Philosophical*

1176   *Society* **126**:1–211.

1177   Carroll RL, Holmes R. 1980. The skull and jaw musculature as guides to the ancestry of

1178   salamanders. *Zoological Journal of the Linnean Society* **68**:1–40. DOI: 10.1111/j.1096-

1179   3642.1980.tb01916.x

1180   Chen J, Gao KQ. 2009. Early Cretaceous hynobiid *Liaoxitriton zhongjiani* (Amphibia: Caudata)

1181   from Liaoning, China, and the monophyly of the Hynobiidae. *Journal of Vertebrate*

1182   *Paleontology* **29** (supplement to no. 3):76A. DOI: 10.1080/02724634.2009.10411818.

1183   Chen MY, Mao RL, Liang D, Kuro-o M, Zeng XM, Zhang P. 2015. A reinvestigation of

1184   phylogeny and divergence times of Hynobiidae (Amphibia, Caudata) based on 29 nuclear

1185   genes. *Molecular Phylogenetics and Evolution* **83**:1–6. DOI:

1186   10.1016/j.ympev.2014.10.010.

1187   Cloete SE. 1961. The cranial morphology of *Rhyacotriton olympicus olympicus* (Gaige). *Annals*

1188   *of the University of Stellenbosch* **36A**:113–145.

1189   Cope ED. 1859. On the primary divisions of the Salamandridae, with descriptions of two new

1190   species. *Proceedings of the Academy of Natural Sciences of Philadelphia* **11**:122–128.

1191   David A. 1872 (1871). Rapport adressé a MM. les Professeur-Administráteurs du Museum

1192   d'histoire naturelle. *Nouvelles Archives du Muséum d'Histoire Naturelle*. Paris **7**:75–100.

1193   De Beer GR. 1937. *The Development of the Vertebrate Skull*. Oxford: the Clarendon Press.

1194   Duellman WE, Trueb L. 1986. *Biology of Amphibians*. New York: McGraw-Hill Book

1195   Company.

1196   Duméril AMC. 1806. *Zoologie analytique, ou méthode naturelle de classification des animaux,*

1197   *rendue plus facile à l'aide de tableaux synoptiques*. Paris: Allais.

1198   Dunn ER. 1922. The sound-transmitting apparatus of salamanders and the phylogeny of the

1199   Caudata. *American Naturalist* **56**:418–427. DOI 10.1086/279882.

1200   Dunn ER. 1923. The salamanders of the family Hynobiidae. *Proceedings of the American*

1201   *Academy of Arts and Sciences* **58**:445–523. DOI: 10.2307/20026019.

1202   Edwards JL. 1976. Spinal nerves and their bearing on salamander phylogeny. *Journal of*

1203   *Morphology* **148**:305–328. DOI: 10.1002/jmor.1051480304.

1204   Elwood JRL, Cundall D. 1994. Morphology and behavior of the feeding apparatus in

1205   *Cryptobranchus alleganiensis* (Amphibia: Caudata). *Journal of Morphology* **220**: 47–70.

1206   DOI: 10.1002/jmor.1052200106.

1207   Erdman S, Cundall D. 1984. The feeding apparatus of the salamander *Amphiuma tridactylum*:

1208   morphology and behavior. *Journal of Morphology* **181**:175–204.

1209   Estes R. 1981. *Encyclopedia of Paleoherpetology*, *Part 2: Gymnophiona*, *Caudata*. Stuttgart:

1210   Gustav Fischer Verlag.

1211   Fei L, Ye C. 1983. Systematic studies on Hynobiidae, including diagnosis of a new genus

1212   *Pseudohynobius* (Amphibia: Caudata). *Acta Herpetologica Sinica* **2**: 31–37. (in Chinese

1213   with English abstract).

1214   Fei L, Ye C. 1984. On the geographical-distribution, center of differentiation and phylogenetic-

1215   relationships of the different genera of Hynobiidae (Amphibia, Salamandriformes). *Acta*

1216   *Zoologica Sinica* **30**:385–392. (in Chinese with English abstract).

1217   Fei L, Ye C. 2001. *The Color Handbook of the Amphibians of Sichu*an. Chengdu, China: Sichuan

1218   Forestry Department, Sichuan Association of Wildlife Conservation, and Chengdu

1219   Institute of Biology.

1220   Fei L, Ye C. 2017. Amphibians of China (Vol. I). Beijing: Science Press.

1221   Fei L, Ye C, Tian W. 1983. Systematic discussion on the genus *Batrachuperus* with description

1222   of a new species. *Acta Zootaxonomica Sinica* **8**:209–219. (in Chinese with English

1223   abstract).

1224   Fei L, Hu S, Ye C, Huang Y. 2006. *Fauna Sinica Amphibia volume 1*. Beijing: Science Press (in

1225   Chinese with English abstract).

1226   Fei L, Ye C, Jiang J. 2010. *Colored Atlas of Chinese Amphibians*. Chengdu: Sichuan Publishing

1227   Group.

1228   Fei L, Ye C, Jiang J. 2012. *Colored Atlas of Chinese Amphibians and Their Distributions*.

1229   Chengdu: Sichuan Publishing Group.

1230   Fox H. 1959. A study of the development of the head and pharynx of the larval urodele *Hynobius*

1231   and its bearing on the evolution of the vertebrate head. *Philosophical transactions of the*

1232   *Royal Society of London. Series B, Biological Sciences* **242**:151–204. URL:

1233   http://www.jstor.org/stable/2992618.

1234   Francis ETB. 1934. *The Anatomy of the Salamander*. Oxford: Clarendon Press.

1235   Frost DR. 2017. Amphibian Species of the World: an Online Reference. Version 6.0. (accessed 4

1236   March 2017). Electronic Database accessible at

1237   http://research.amnh.org/herpetology/amphibia/index.html. American Museum of Natural

1238   History, New York, USA.

1239   Fu J, Zeng X. 2008. How many species are in the genus *Batrachuperus*? A phylogeographical

1240   analysis of the stream salamanders (family Hynobiidae) from southwestern China.

1241   *Molecular Ecology* **17**(6):1469–1488. DOI: 10.1111/j.1365-294X.2007.03681.x.

1242 Fu J, Wang Y, Zeng X, Liu Z, Zheng Y. 2001. Genetic diversity of Eastern *Batrachuperus*

1243   (Caudata: Hynobiidae). *Copeia* **2001 (4)**:1100–1107. DOI: 10.1643/0045-

1244   8511(2001)001[1100:GDOEBC]2.0.CO;2.

1245 Fukuda Y. 1930. Die Veränderungen des Hyobranchialskeletts vom *Onychodactylus japonicus*

1246   bei der Metamorphose. *Folia Anatomica Japonica* **9**:47–72.

1247 Gao KQ, Shubin NH. 2001. Late Jurassic salamanders from northern China. *Nature* **410**:574–

1248   577. DOI: 10.1038/35069051.

1249 Gao KQ, Shubin NH. 2003. Earliest known crown-group salamanders. *Nature* **422**:424–428.

1250   DOI: 10.1038/nature01491.

1251 Gao KQ, Shubin HN. 2012. Late Jurassic salamandroid from western Liaoning, China.

1252   *Proceedings of the National Academy of Sciences of the United States of America*

1253   **109**:5767–5772. DOI: 10.1073/pnas.1009828109.

1254 Gao KQ, Chen J, Jia J. 2013. Taxonomic diversity, stratigraphic range, and exceptional

1255   preservation of Juro-Cretaceous salamanders from northern China. *Canadian Journal of*

1256   *Earth Sciences* **50**:255–267. DOI: 10.1139/e2012-039.

1257 Gaupp E. 1898. Ontogenese und Phylogenese des schalleitenden Apparates bei den Wirbeltieren.

1258   *Ergebnisse der Anatomie und Entwicklungsgeschichte* **VIII**:990–1149.

1259 Gaupp E. 1911. Über den N. trochlearis der Urodelen und über die Austrittsstellen der

1260   Gehirnnerven aus dem Schädelraum im allgemeinen. *Anatomischer Anzeiger* **38**:401–

1261   444.

1262 Goodrich ES. 1930. *Studies on the Structure and Development of Vertebrates*. Chicago: The

1263   University of Chicago Press.

1264   Hanken J, Wassersug R. 1981. The visible skeleton: A new double-stain technique reveals the

1265   nature of the "hard" tissues. *Functional Photography* **16**:22–26.

1266   Hecht MK, Edwards JL. 1976. The determination of parallel or monophyletic relationships: the

1267   proteid salamanders- a test case. *The American Naturalist* **110**:653–677. DOI:

1268   10.1086/283096.

1269   Hecht MK, Edwards JL. 1977. The methodology of phylogenetic inference above the species

1270   level. In: Hecht MK, Goody PC, Hecht BM, eds. *Major Patterns in Vertebrate Evolution*,

1271   New York and London: Plenum Press, 3–51.

1272   Inukai T. 1930-1932. Urodelenarten aus Nord Japan mit besonderer Berüucksichtigung der

1273   Morphologie des Schädels. *Journal of the Faculty of Science, Hokkaido University,*

1274   *Series 6 Zoology* **1**:191–217.

1275   ICZN, 1999. International Code of Zoological Nomenclature. 4th edition, published by the

1276   international Trust for Zoological Nomenclature 1999.

1277   IUCN, 2016. *The IUCN Red List of Threatened Species*. Version 2016-2. www.iucnredlist.org.

1278   Downloaded on 30 October 2016.

1279   Ivachnenko M. 1978. Urodeles from the Triassic and Jurassic of Soviet Central Asia.

1280   *Paleontological Journal* **1978**:362–368.

1281   Jia J, Gao KQ. 2016a. A new hynobiid-like salamander (Amphibia, Urodela) from Inner

1282   Mongolia, China, provides a rare case study of developmental features in an Early

1283   Cretaceous fossil urodele. *PeerJ* **4**:e2499; DOI: 10.7717/peerj.2499.

1284   Jia J, Gao KQ. 2016b. A new basal salamandroid (Amphibia, Urodela) from the Late Jurassic of

1285   Qinglong, Hebei Province, China. *PLoS ONE* **11**:e0153834. DOI:

1286   10.1371/journal.pone.0153834.

1287   Jiang Z, Jiang J, Wang Y, Zhang E, Zhang Y, Li L, Xie F, Cai B, Cao L, Zheng G, Dong L,

1288   Zhang Z, Ding P, Luo Z, Ding C, Ma Z, Tang S, Cao W, Li C, Hu H, Ma Y, Wu Y,

1289   Wang Y, Zhou K, Liu S, Chen Y, Li J, Feng Z, Wang Y, Wang B, Li C, Song X, Cai L,

1290   Zang C, Zeng Y, Meng Z, Fang H, Ping X. 2016. Red list of China's vertebrates.

1291   *Biodiversity Science* **24**:500–553.

1292   Jömann N, Clemen G, Greven H. 2005. Notes on cranial ontogeny and delayed metamorphosis

1293   in the hynobiid salamander *Ranodon sibiricus* Kessler, 1866 (Urodela). *Annals of*

1294   *Anatomy* **187**:305–431. DOI: 10.1016/j.aanat.2005.02.010.

1295   Kami HG. 1999. Additional specimens of the Persian Mountain Salamander, *Batrachuperus*

1296   *persicus*, from Iran (Amphibia: Hynobiidae). *Zoology in the Middle East* **19(1)**:37–42.

1297   DOI: 10.1080/09397140.1999.10637794. url:

1298   http://dx.doi.org/10.1080/09397140.1999.10637794

1299   Kingsbury BF, Reed HD. 1909. The columella auris in Amphibia. Second Contribution. *Journal*

1300   *of Morphology* **20**:549–628. DOI: 10.1002/jmor.1050200403.

1301   Laboratory of Amphibians and Reptiles, Biological Institute of Sichuan Province. 1977. *A*

1302   *Systematic Checklist of Chinese Amphibians*. Beijing: Science Press, 1–97. (in Chinese)

1303   Larson, JHJ, Beneski JTJ, Miller BT. 1996. Structure and function of the hyolingual system in

1304   *Hynobius* and its bearing on the evolution of prey capture in terrestrial salamanders.

1305   *Journal of Morphology* **227**:235–248. DOI: 10.1002/(SICI)1097-

1306   4687(199602)227:2<235:AID-JMOR>3.0.CO;2-7.

1307   Lebedkina NS. 1964. The development of the dermal bones of the basement of the skull in

1308   Urodela (Hynobiidae). *Trudy Akademiia Nauk SSSR* **33**:75–172.

1309   Lebedkina NS. 2004. *Evolution of the Amphibian Skull*. Moscow: Pensoft Publishers.

1310   Litvinchuk SN, Borkin LJ. 2003. Variation in number of trunk vertebrae and in count of costal

1311   grooves in salamanders of the family Hynobiidae. *Contributions to Zoology* **72**: 195–209.

1312   url: http://dpc.ubs.uva.nl/vol72/nr04/a01

1313   Liu CC. 1950. Amphibians of Western China. *Chicago Natural History Museum Fieldiana*

1314   *Zoology Memoirs* **2**:1–400.

1315   Liu CC, Tian WS. 1978. In Liu CC, Hu SQ, Tian WS, Wu GF. 1978: Four new amphibian

1316   species from Sichuan and Guangxi. *Materials for Herpetological Research Chengdu*

1317   **4**:18–19.

1318   Liu CC, Tian WS. 1983. In Fei L, Ye CY, Tian WS. 1983: Systematic discussion of the genus

1319   *Batrachuperus* with description of a new species (Salamandriformes, Hynobiidae). *Acta*

1320   *Zootaxonomica Sinica* **8**:209–219. (in Chinese with English abstract)

1321   Monath T. 1965. The opercular apparatus of salamanders. Journal of Morphology **116**:149–170.

1322   DOI: 10.1002/jmor.1051160202.

1323   Morescalchi A. 1973. Amphibia. In: Chiarelli AB, Capanna E, eds. *Cytotaxonomy and*

1324   *Vertebrate Evolution*. New York and London: Academic Press, 233–348.

1325   Morescalchi A. 1975. Chromosome evolution in the caudate Amphibia. *Evolutionary Biology*

1326   **8**:339–387.

1327   Noble GK. 1931. *The Biology of the Amphibia*. New York and London: McGraw-Hill Book

1328   Company.

1329   Okajima K, Tsuaki T. 1921. Beiträge zur Morphologie des Skleralknorpels bei den Urodelen.

1330   *Zeitschrift für Anatomie und Entwicklungsgeschichte* **60**: 631–651.

1331   Olson EC. 1966. The middle ear—morphological types in amphibians and reptiles. *American*

1332   *Zoologist* **6**:399–419. DOI: https://doi.org/10.1093/icb/6.3.399.

1333   Reese AM. 1906. Anatomy of *Cryptobranchus allegheniensis*. *The American Naturalist* **40**:287–

1334   326. DOI: https://doi.org/10.1086/278619.

1335   Regel ED. 1970. Ascending process of the palatoquadratic cartilage in urodelans. *Doklady*

1336   *Akademii Nauk SSSR* **194**:509–512.

1337   Reilly SM. 1983. The biology of the high altitude salamander *Batrachuperus mustersi* from

1338   Afghanistan. *Journal of Herpetology* **17**:1–9. DOI: 10.2307/1563774.

1339   Reilly SM. 1987. Ontogeny of the hyobranchial apparatus in the salamanders *Ambystoma*

1340   *talpoideum* (Ambystomatidae) and *Notophthalmus viridescens* (Salamandridae): the

1341   ecological morphology of two neotenic strategies. Journal of Morphology **191**:205–214.

1342   DOI: 10.1002/jmor.1051910210.

1343   Reilly SM, Altig R. 1996. Cranial ontogeny in *Siren intermedia* (Caudata: Sirenidae):

1344   paedomorphic, metamorphic, and novel patterns of heterochrony. *Copeia* **1996**:29–41.

1345   DOI: 10.2307/1446939.

1346   Reilly SM, Lauder G. 1988. Atavisms and the homology of hyobranchial elements in lower

1347   vertebrates. *Journal of Morphology* **195**:237–245.

1348   Rose CS. 2003. The developmental morphology of salamander skulls. In: Heatwole H, Davies

1349   M, eds. *Amphibian Biology. Volume 5: Osteology*. Chipping Norton NSW: Surrey Beatty

1350   & Sons, 1684–1781.

1351   Sasaki M. 1924. On a Japanese salamander, in Lake Kutarush, which propagates like the axolotl.

1352   *Journal of the College of Agriculture, Hokkaido Imperial University* **15**:1–36.

1353   Sato I. 1943. *A Monograph of the Tailed Batrachians of Japan*. Osaka: Nippon Shuppan-sha.

1354   Sessions SK. 2008. Evolutionary cytogenetics in salamanders. *Chromosome Research* **16**:183–

1355   201. DOI:10.1007/s10577-007-1205-3.

1356   Schmalhausen II. 1958. Nasolacrimal duct and septomaxillare of Urodela. *Zoologicheskii*

1357   *Zhurnal* **37**:570–583.

1358   Schmalhausen II. 1968. *The Origin of Terrestrial Vertebrates*. New York: Academic Press.

1359   Shubin NH, Wake DB. 2003. Morphological variation, development, and evolution of the limb

1360   skeleton of salamanders. In: Heatwole H, Davies M, eds. *Amphibian Biology. Volume 5:*

1361   *Osteology*. New South Wales: Surrey Beatty and Sons, 1782–1808.

1362   Smirnov SV, Vassilieva AB. 2002. Skeletal and dental ontogeny in the long-tailed clawed

1363   salamander, *Onychodactylus fischeri* (Urodela: Hynobiidae). *Russian Journal of*

1364   *Herpetology* **9**:21–32. URL: http://rjh.folium.ru/index.php/rjh/article/view/590.

1365   Song M, Zeng X, Wu G, Liu Z, Fu J. 2001. A new species of *Batrachuperus* from northwestern

1366   China. *Asiatic Herpetological Research* **9**:6–8. DOI: 10.5962/bhl.part.15559.

1367   Sparreboom M. 2014. *Salamanders of the Old World*. Zeist: KNNV Publishing.

1368   Suzuki T. 1932. Development of the brain, nervous system, and cranial skeleton in amphibians.

1369   I. Development of the skull in *Onychodactylus japonicus*. *Kaibogaku Zassi* (*Acta*

1370   *Anatomica Japonica*) **5**:685–719.

1371   Trueb L. 1993. Patterns of cranial diversity among the Lissamphibia. In: Hanken J, Hall BK, eds.

1372   *The Skull, Volume 2: Patterns of Structural and Systematic Diversity*. Chicago: The

1373   University of Chicago Press, 255–343.

1374   Trueb L, Cloutier R. 1991. A phylogenetic investigation into the inter- and intrarelationships of

1375   the Lissamphibia (Amphibia: Temnospondyli). In: Schultze HP, Trueb L, eds. *Origins of*

1376   *the Higher Groups of Tetrapods: Controversy and Consensus*. Ithaca and London:

1377   Cornell University Press, 223–231.

1378   Vassilieva AB, Poyarkov NA, Iizuka K. 2013. Pecularities [sic] of bony skeleton development in

1379   Asian clawed salamanders (*Onychodactylus*, Hynobiidae) related to embryonization.

1380   *Biology Bulletin* **40**:1–11. 589–599. DOI: 10.1134/S1062359013070078.

1381   Vassilieva AB, Lai JS, Yang SF, Chang YH, Poyarkov NA. Jr. 2015. Development of the bony

1382   skeleton in the Taiwan salamander, *Hynobius formosanus* Maki, 1922 (Caudata:

1383   Hynobiidae): heterochronies and reductions. *Vertebrate Zoology* **65**:117–130.

1384   Wakahara M. 1996. Heterochrony and neotenic salamanders: possible clues for understanding

1385   the animal development and evolution. *Zoological Science* **13**:756–766.

1386   Wake DB. 2001. "*Dicamptodon ensatus*" (On-line), Digital Morphology. Accessed April 5, 2017

1387   at http://digimorph.org/specimens/*Dicamptodon_ensatus*/.

1388   Whipple I. 1906. The ypsiloid apparatus of urodeles. *The Biological Bulletin* **10**:255–297.

1389   Worthington RD, Wake DB. 1971. Larval morphology and ontogeny of the ambystomatid

1390   salamander, *Rhyacotriton olympicus*. *American Midland Naturalist* **85**:349–365. DOI: 27

1391   10.2307/2423762.

1392   Wu C. 1982. External and skeletal anatomy of *Meglobatrachus davidianus*. *Journal of Zoology*

1393   **17**:11–16. (in Chinese)

1394   Wu G, Xie F. 2004. *Batrachuperus londongensis*. The IUCN Red List of Threatened Species

1395   2004: e.T59084A11867916.

1396   http://dx.doi.org/10.2305/IUCN.UK.2004.RLTS.T59084A11867916.en. Downloaded on

1397   01 January 2017.

1398   Xiong JL, Yu P, Zhang JL, Zhu WW, Sun P. 2013a. Vertebral column characteristics of

1399   *Batrachuperus pinchonii*, and discussion on the division of the vertebral column in

1400   Urodela. *Chinese Journal of Zoology* **48**:451–456. (in Chinese with English abstract).

1401   Xiong JL, Sun P, Zhang JL, Liu XY. 2013b. A comparative study of the hyobranchial apparatus

1402   in Hynobiidae (Amphibia: Urodela). *Zoology* **116**:99–105. DOI:

1403   10.1016/j.zool.2012.10.004.

1404   Zhang F. 1985. On anatomy of the skeletal system of *Liua shihi* (Liu) (Amphibia: Hynobiidae).

1405   *Acta Herpetologica Sinica* **4**:17–24. (in Chinese with English abstract)

1406   Zhang H, Liu S, Zhao Y, Yang Q. 2009. Skeletal system of *Batrachuperus pinchonii*. *Sichuan*

1407   *Journal of Zoology* **28**:412–416. (in Chinese with English abstract)

1408   Zhang P. Chen YQ, Zhou H, Liu Y-F, Wang L, Papenfuss TJ, Wake DB, Qu L-H. 2006.

1409   Phylogeny, evolution, and biogeography of Asiatic salamanders (Hynobiidae).

1410   *Proceedings of the National Academy of Sciences of the United States of America*

1411   **103**:7360–7365. DOI: 10.1073/pnas.0602325103.

1412   Zheng Y, Peng R, Kuro-o M, Zeng X. 2011. Exploring patterns and extent of bias in estimating

1413   divergence time from mitochondrial DNA sequence data in a particular lineage: a case

1414   study of salamanders (Order Caudata). *Molecular Biology and Evolution* **28**:2521–2535.

1415   DOI: 10.1093/molbev/msr072.

1416

1417   **Figure Captions**

1418

1419   Figure 1. Photographs of ethanol-preserved specimens of *Batrachuperus londongensis* in dorsal

1420   view: (A) holotype CIB 65I0013/14380; (B) referred specimen CIB 14381; (C) referred

1421   specimen CIB 14504. All topotypic specimens were collected from the type locality Longdong

1422   Stream, Mt. Emei, Sichuan Province, China.

1423

1424   Figure 2. Skull roof of *Batrachuperus londongensis*: (A) holotype CIB 65I0013/14380; (B) CIB

1425   14381; (C) CIB 14482. Specimens CIB 14381 (B) and CIB 14482 (C) display an incomplete

1426   resorption of palatine. Anatomical abbreviations used in this and other figures see list in

1427   Materials & Methods.

1428

1429   Figure 3. Lateral view of the skull of *Batrachuperus londongensis*: (A) holotype CIB

1430   65I0013/14380; (B) CIB 14381; (C) CIB 14482. Specimens CIB 14381 (B) and CIB 14482 (C)

1431   display an incomplete resorption of palatine. All images with squamosal and quadrate removed

1432   to expose the otic capsule. Note the unusual perichondral ossification of the ascending process of

1433   palatoquadrate as a pillar between the parietal and pterygoid anterior to the prootic.

1434

1435   Figure 4. Palatal view of the skull of *Batrachuperus londongensis*: (A) holotype CIB

1436   65I0013/14380; (B) CIB 14381; (C) CIB 14482. Specimens CIB 14381 (B) and CIB 14482 (C)

1437   display an incomplete resorption of palatine. All specimens show that the two vomers have no

1438   midline contact behind the anteromedial fenestra.

1439

1440 Figure 5. Mandible of *Batrachuperus londongensis*: right mandible of CIB 14482 in medial (A)

1441 and lateral (B) views; mandibular arch of CIB 14482 in dorsal (C) and ventral (D) views.

1442

1443 Figure 6. Hyobranchial apparatus of *Batrachuperus londongensis*: (A) CIB 14499, showing a

1444 neotenic pattern with extra ceratobranchials III and IV; (B) CIB 14504, showing a

1445 postmetamorphic pattern with ceratobranchials III and IV entirely lost by resorption.

1446

1447 Figure 7. Holotype skeleton of *Batrachuperus londongensis* (CIB 65I0013/14380): 3D

1448 reconstruction of whole body of the holotype skeleton in dorsal (A) and ventral (B) views.

1449

1450 Figure 8. Pectoral girdle and upper arm of *Batrachuperus londongensis*: CIB 65I0013/14380, left

1451 scapulocoracoid in lateral (A) and lateroventral (B) views; left scapulocoracoid of CIB 14381 in

1452 lateral (C) and lateroventral (D) views; left scapulocoracoid of CIB 14504 in lateral (E) and

1453 lateroventral (F) views; left humerus of CIB 65I0013/14380 in dorsal (G) and ventral (H) views;

1454 right humerus of CIB 14381 in dorsal (I) and ventral (J) views; left humerus of CIB 14504 in

1455 dorsal (K) and ventral (L) views. Note unusual ossification of normally cartilaginous parts of

1456 procoracoid and coracoid in the holotype (A, B) and CIB 14504 (E, F). All images not to scale.

1457

1458 Figure 9. Left forearm of *Batrachuperus londongensis*: (A) CIB 14381; (B) CIB 14484; (C) CIB

1459 14487; (D) CIB 14507. All images display presence of direct contact of the centrale with radius

1460 as an unusual feature in urodeles. All in dorsal view and not to scale.

1461

1462   Figure 10. Pelvis and femur of *Batrachuperus londongensis*: Pelvis of CIB 65I0013/14380 in

1463   right lateral (A) and ventral (B) views; pelvis of CIB 14381 in right lateral (C) and ventral (D)

1464   views; pelvis of CIB 14482 in right lateral (E) and ventral (F) views; pelvis of CIB 14487 in

1465   right lateral (G) and ventral (H) views; left femur of CIB 65I0013/14380 in dorsal (I) and ventral

1466   (J) views; left femur of CIB 14381 in dorsal (K) and ventral (L)views; left femur of CIB 14482

1467   in dorsal (M) and ventral (N) views; left femur of CIB 14487 in dorsal (O) and ventral (P) views.

1468   All images not to scale.

1469

1470   Figure 11. Lower hind limb of *Batrachuperus londongensis*: (A) left lower hind limb of CIB

1471   65I0013/14380; (B) left lower hind limb of CIB 14381; (C) left lower hind limb of CIB 14482;

1472   (D) left lower hind limb of CIB 14487. All in dorsal view and not to scale.

1473

1474   Table 1. Measurements of specimens used in this study.

Figure 1

Photographs of ethanol-preserved specimens of *Batrachuperus londongensis* in dorsal view

(A) holotype CIB 65I0013/14380; (B) referred specimen CIB 14381; (C) referred specimen CIB 14504. All topotypic specimens were collected from the type locality Longdong Stream, Mt. Emei, Sichuan Province, China.

Figure 2

Skull roof of *Batrachuperus londongensis*

(A) holotype CIB 65I0013/14380; (B) CIB 143481 (B); (C) CIB 14482. Note Specimens CIB 14381 (B) and CIB 14482 in (C) displaying display an incomplete resorption of palatine. Anatomical abbreviations used in this and other figures see list in Materials & Methods.
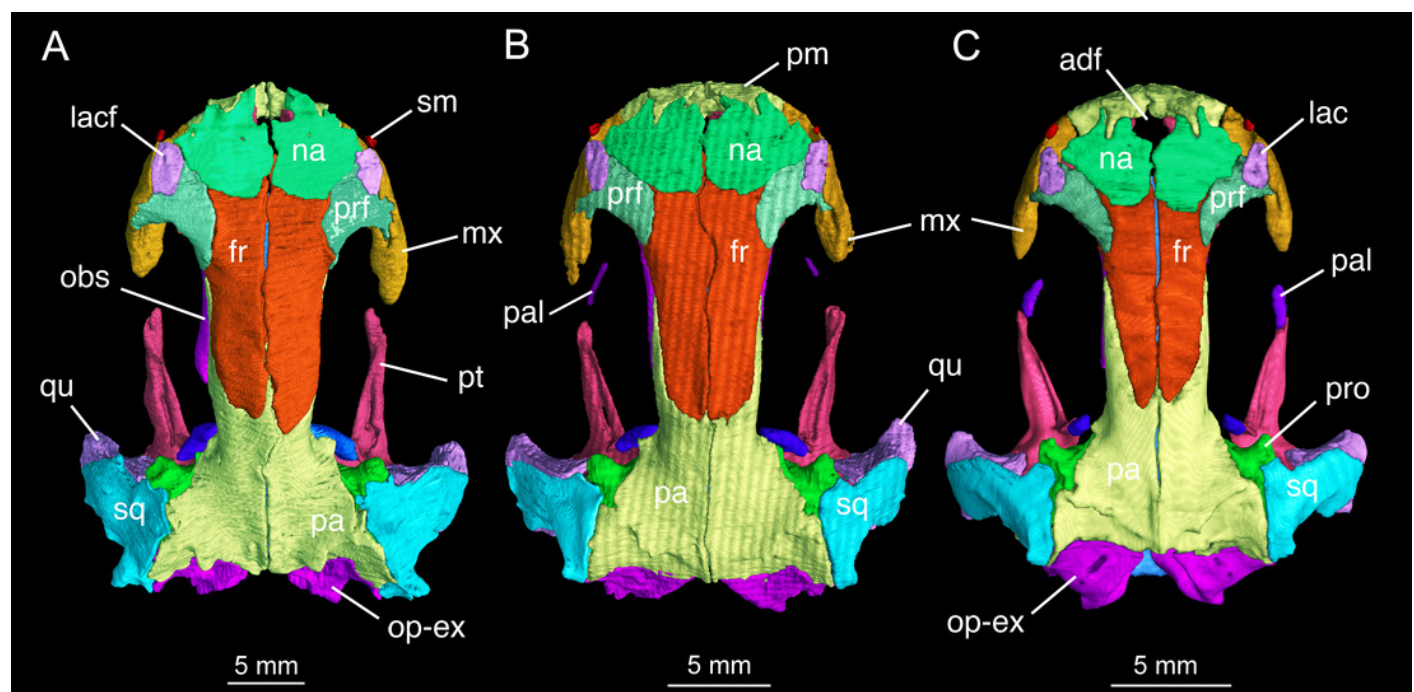
Figure 3

Lateral view of the skull of *Batrachuperus londongensis*

(A) CIB holotype CIB 65I0013/14380; (B) CIB 143481; (C) CIB 14482. Specimens CIB 14381
(B) and CIB 14482 (C) display an incomplete resorption of palatine. All images with
squamosal and quadrate removed to expose the otic capsule. Note the unusual perichondral
ossification of the ascending process of palatoquadrate as a pillar between the parietal and
pterygoid anterior to the prootic.

Note: Auto Gamma Correction was used for the image. This only affects the reviewing manuscript. See original source image if needed for review.
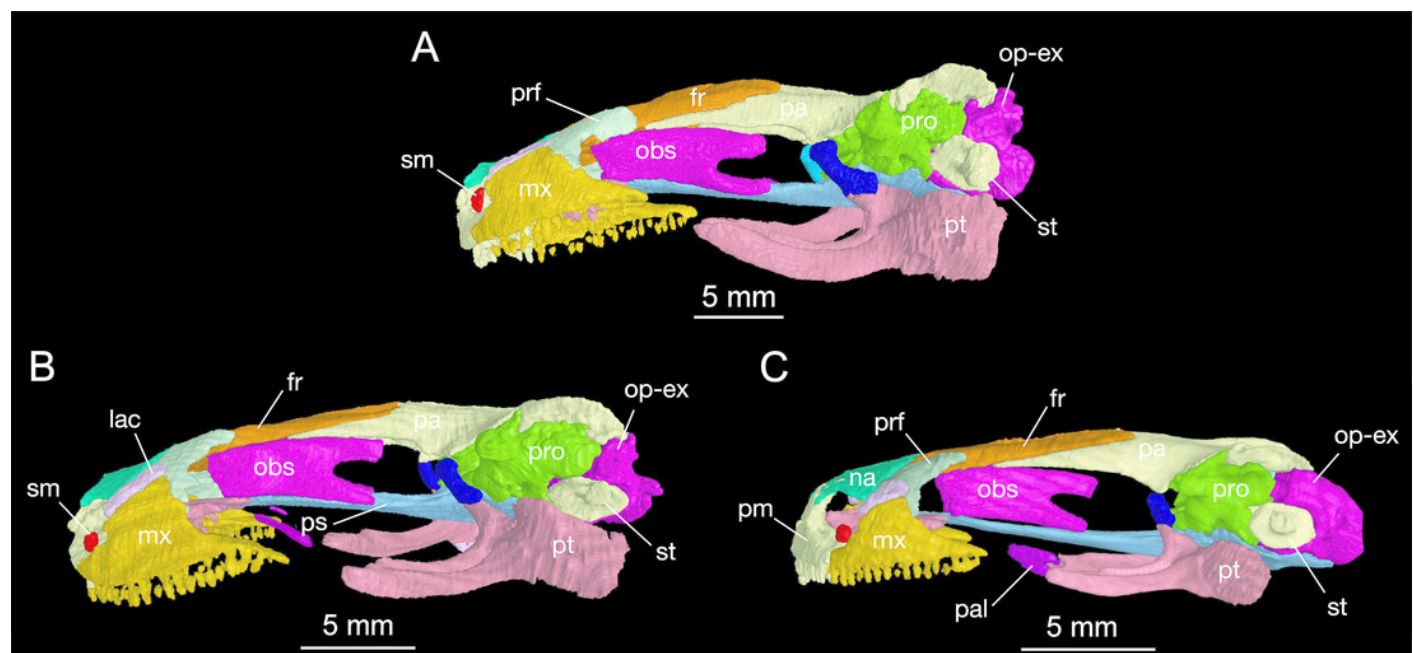
Figure 4

Palatal view of the skull of *Batrachuperus londongensis*

(A) holotype CIB 65I0013/14380; (B) CIB 143481; (C) CIB 14482. Specimens CIB 14381 (B) and CIB 14482 (C) display an incomplete resorption of palatine. NoteAll specimens show that the two vomers have no midline contact behind the anteromedial fenestra.; note also delayed resorption of palatine in CIB 14482 (C).
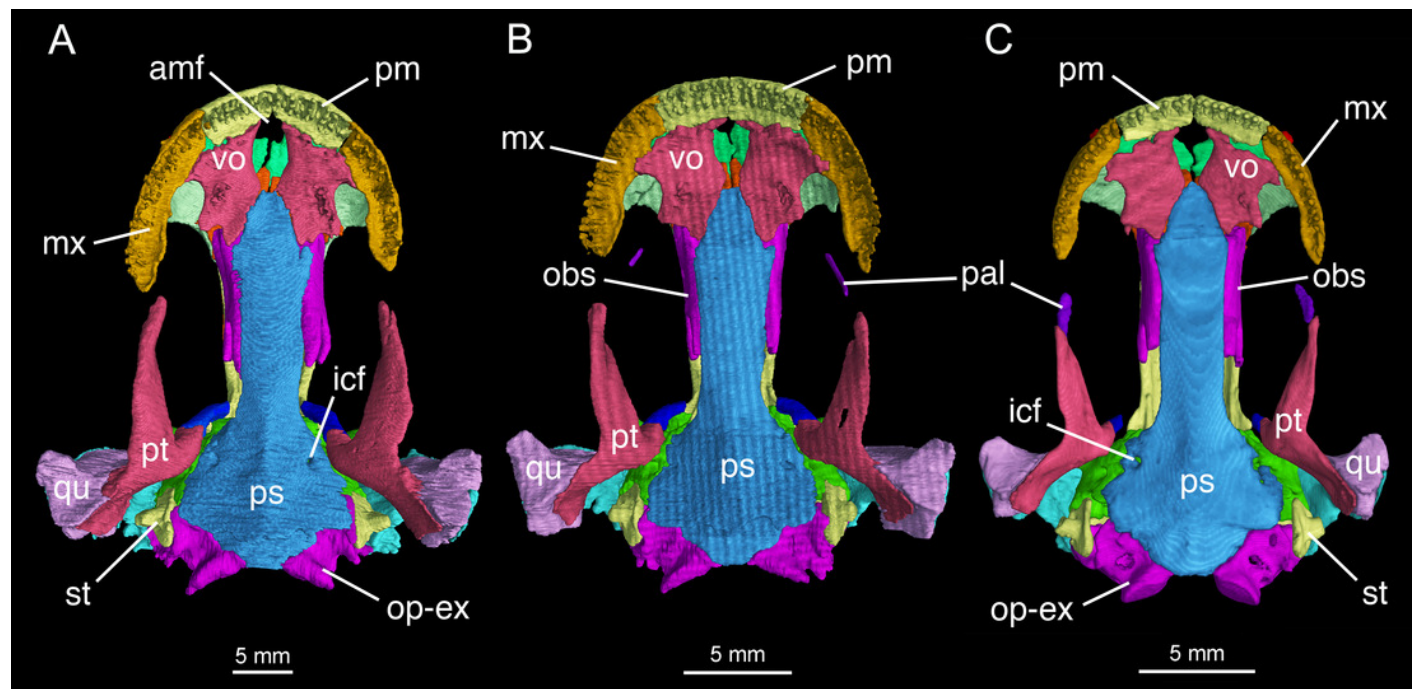
Figure 5

Mandible of *Batrachuperus londongensis*

Right mandible of CIB 14482 in medial (A) and lateral (B) views; mandibular arch of CIB 14482 in dorsal (C) and ventral (D) views.

Note: Auto Gamma Correction was used for the image. This only affects the reviewing manuscript. See original source image if needed for review.
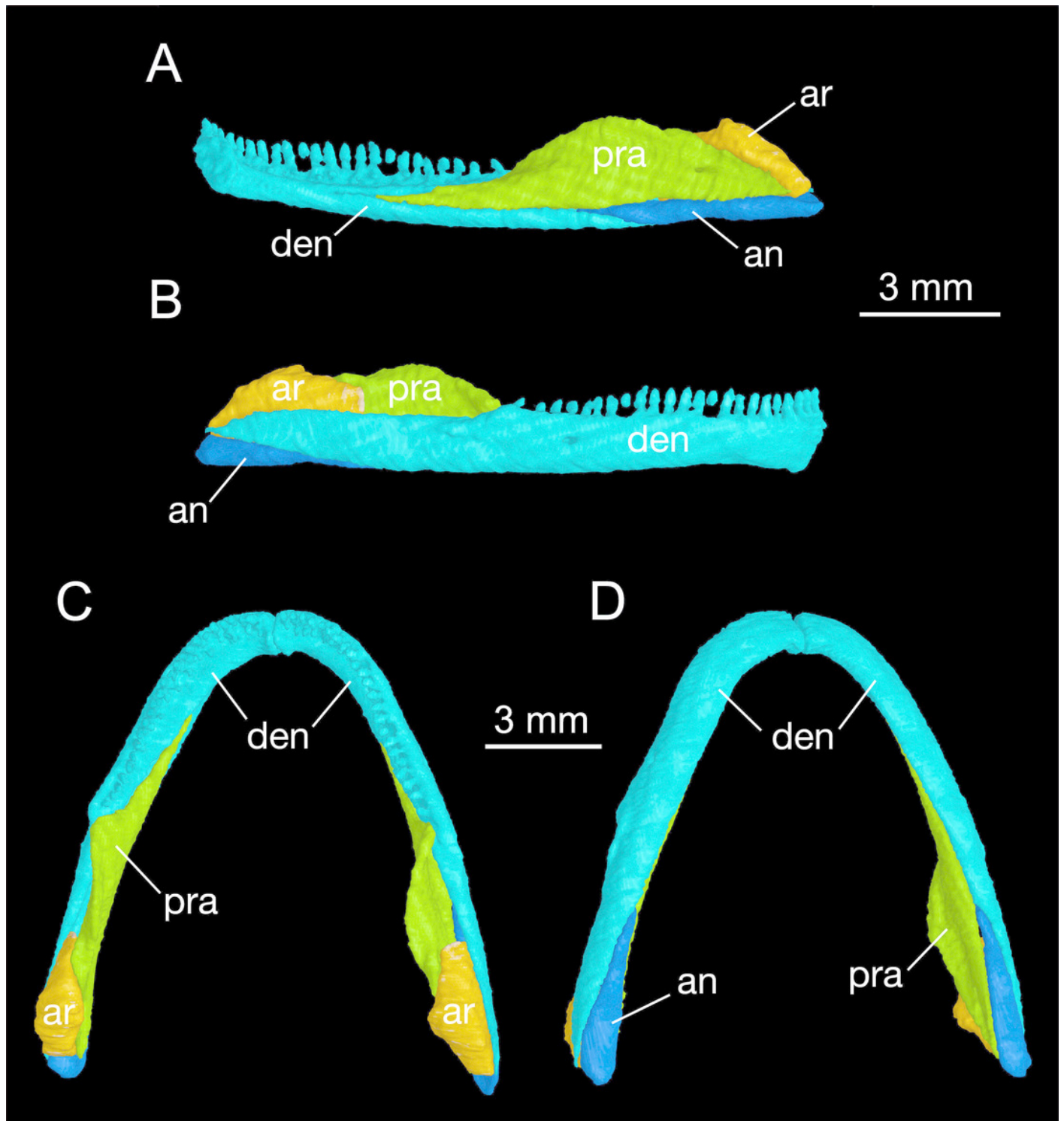
Figure 6

Hyobranchial apparatus of *Batrachuperus londongensis*

(A) CIB 14499, showing a neotenic pattern with extra ceratobranchials III and IV; (B) CIB 14504, showing a postmetamorphic pattern with ceratobranchials III and IV entirely lost by resorption.
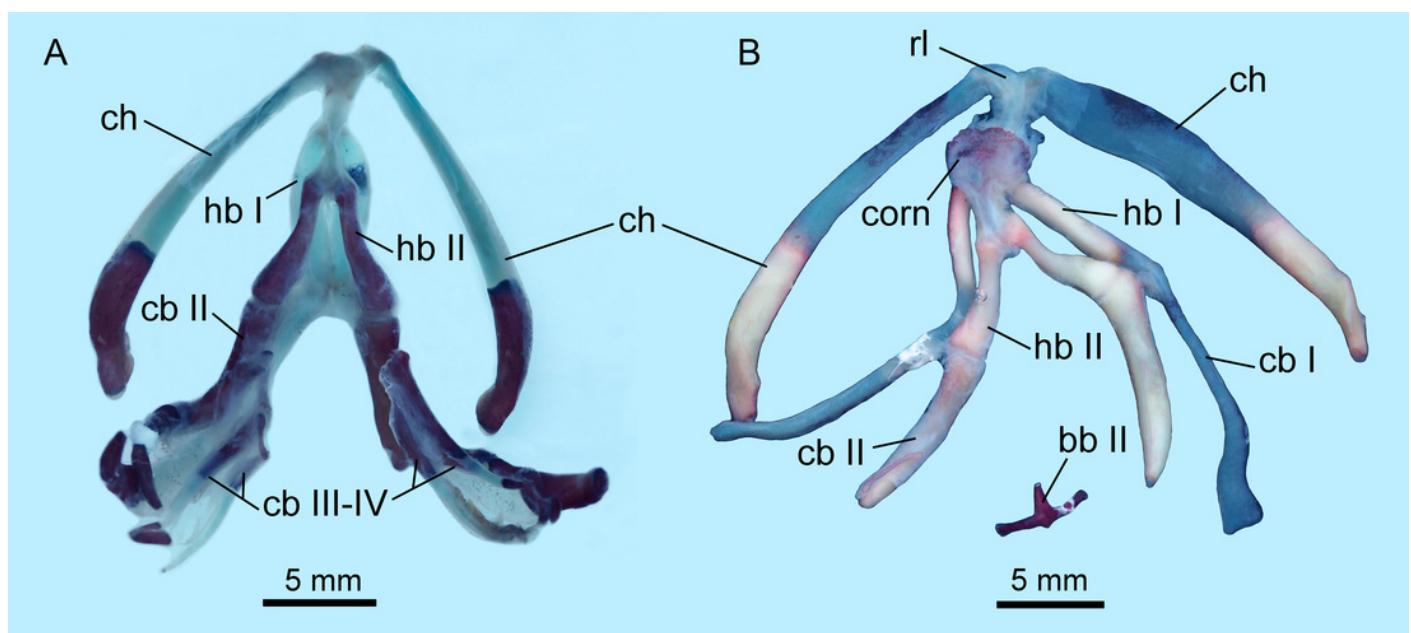
Figure 7

Holotype skeleton of *Batrachuperus londongensis* (CIB 65I0013/14380)

3D reconstruction of whole body of the holotype skeleton in dorsal (A) and ventral (B) views.

Note: Auto Gamma Correction was used for the image. This only affects the reviewing manuscript. See original source image if needed for review.
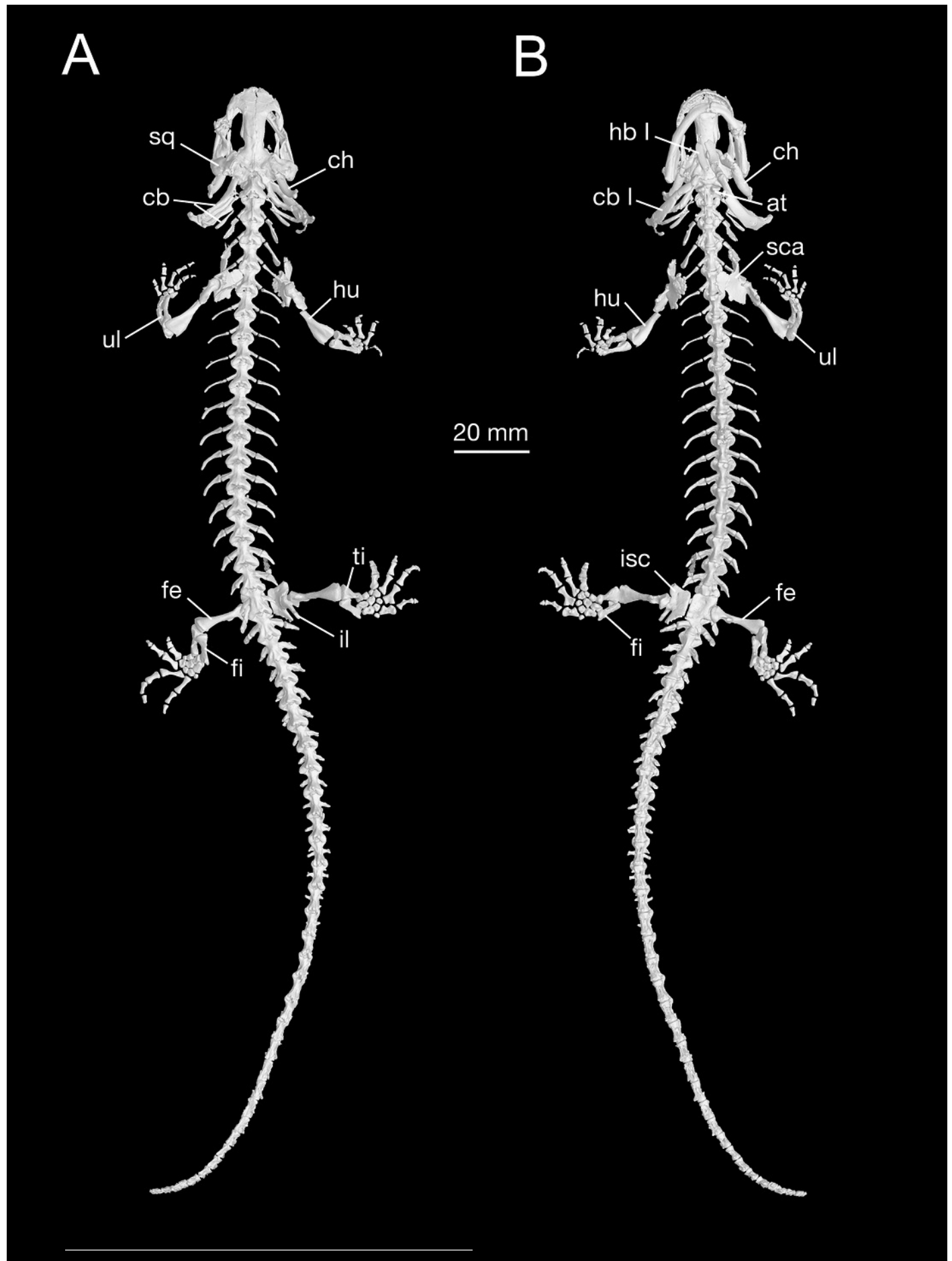
Figure 8

Pectoral girdle and upper arm of *Batrachuperus londongensis*

CIB 65I0013/14380, left scapulocoracoid in lateral (A) and lateroventral (B) views; left scapulocoracoid of CIB 14381 in lateral (C) and lateroventral (D) views; left scapulocoracoid of CIB 14504 in lateral (E) and lateroventral (F) views; left humerus of CIB 65I0013/14380 in dorsal (G) and ventral (H) views; right humerus of CIB 14381 in dorsal (I) and ventral (J) views; left humerus of CIB 14504 in dorsal (K) and ventral (L) views. Note unusual ossification of normally cartilaginous parts of procoracoid and coracoid in the holotype (A, B) and CIB 14504 (E, F). All images not to scale.

Note: Auto Gamma Correction was used for the image. This only affects the reviewing manuscript. See original source image if needed for review.
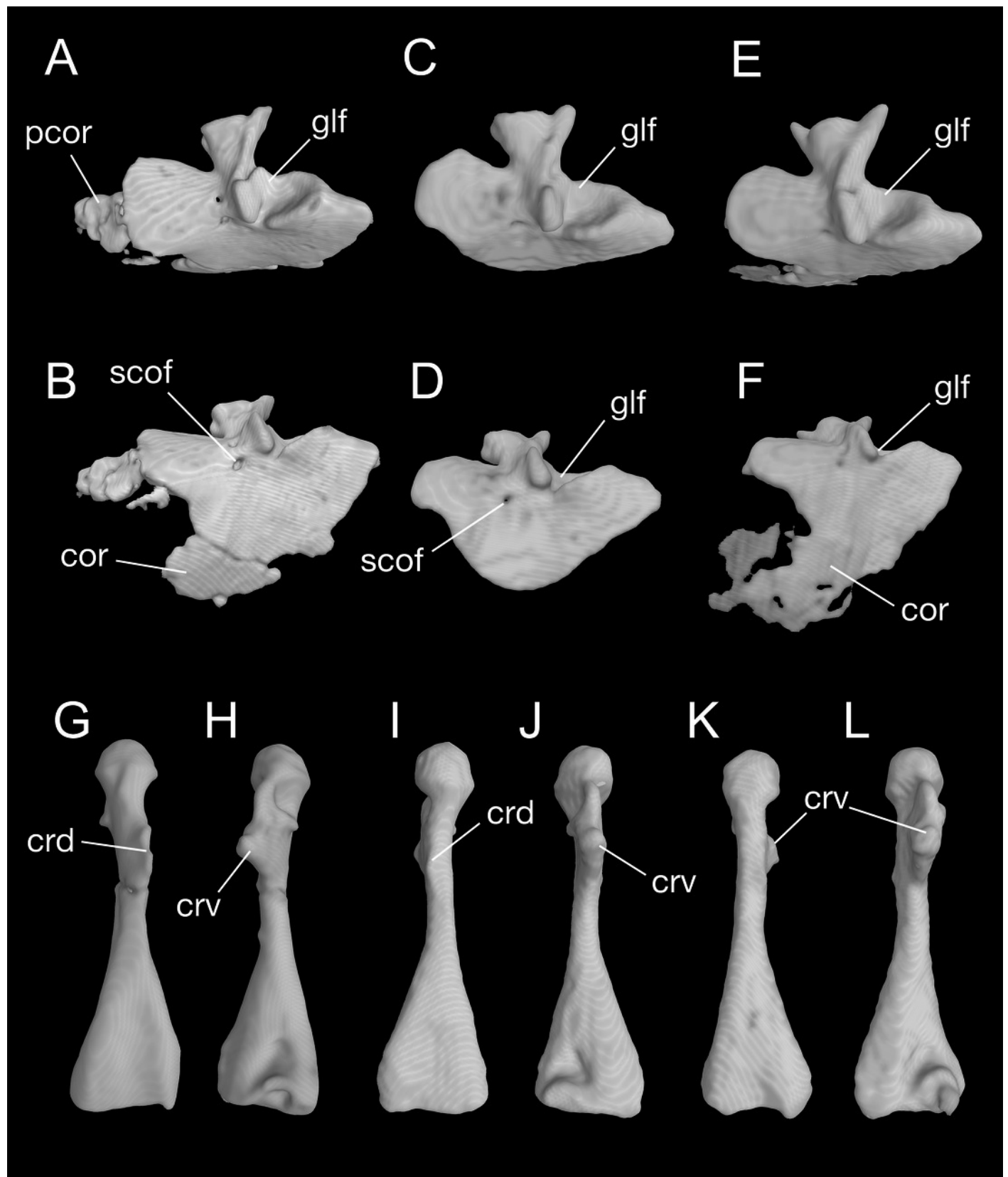
Figure 9

Left forearm of *Batrachuperus londongensis*

(A) CIB 14381; (B) CIB 14484; (C) CIB 14487; (D) CIB 14507. All images display presence of direct contact of the centrale with radius as an unusual feature in urodeles. All in dorsal view and not to scale.

Note: Auto Gamma Correction was used for the image. This only affects the reviewing manuscript. See original source image if needed for review.
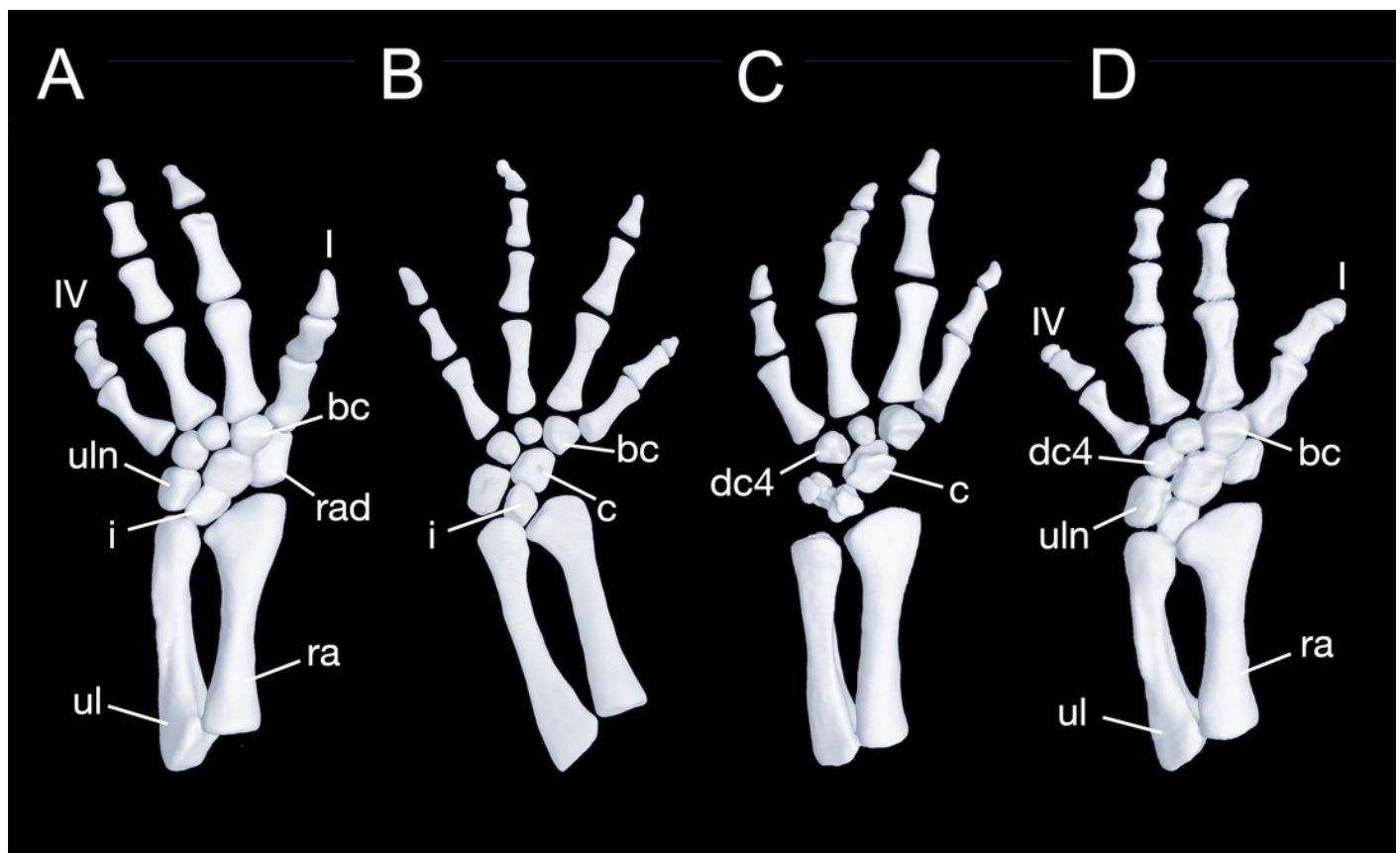
Figure 10

Pelvis and femur of *Batrachuperus londongensis*

Pelvis of CIB 65I0013/14380 in right lateral (A) and ventral (B) views; pelvis of CIB 14381 in right lateral (C) and ventral (D) views; pelvis of CIB 14482 in right lateral (E) and ventral (F) views; pelvis of CIB 14487 in right lateral (G) and ventral (H) views; left femur of CIB 65I0013/14380 in dorsal (I) and ventral (J) views; left femur of CIB 14381 in dorsal (K) and ventral (L)views; left femur of CIB 14482 in dorsal (M) and ventral (N) views; left femur of CIB 14487 in dorsal (O) and ventral (P) views. All images not to scale.
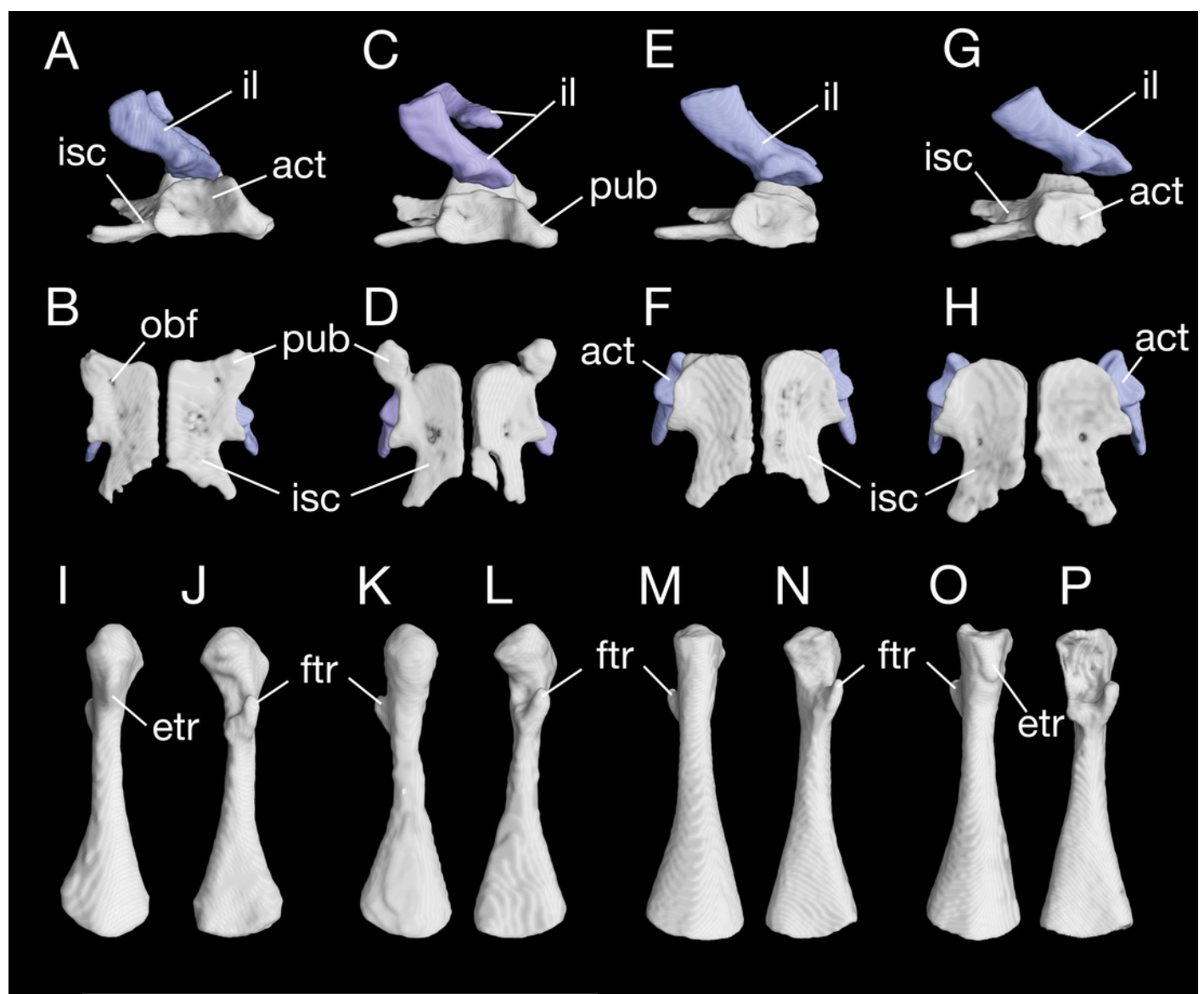
Figure 11

Lower hind limb of *Batrachuperus londongensis*

(A) left lower hind limb of CIB 65I0013/14380; (B) left lower hind limb of CIB 14381; (C) left lower hind limb of CIB 14482; (D) left lower hind limb of CIB 14487. All in dorsal view and not to scale.
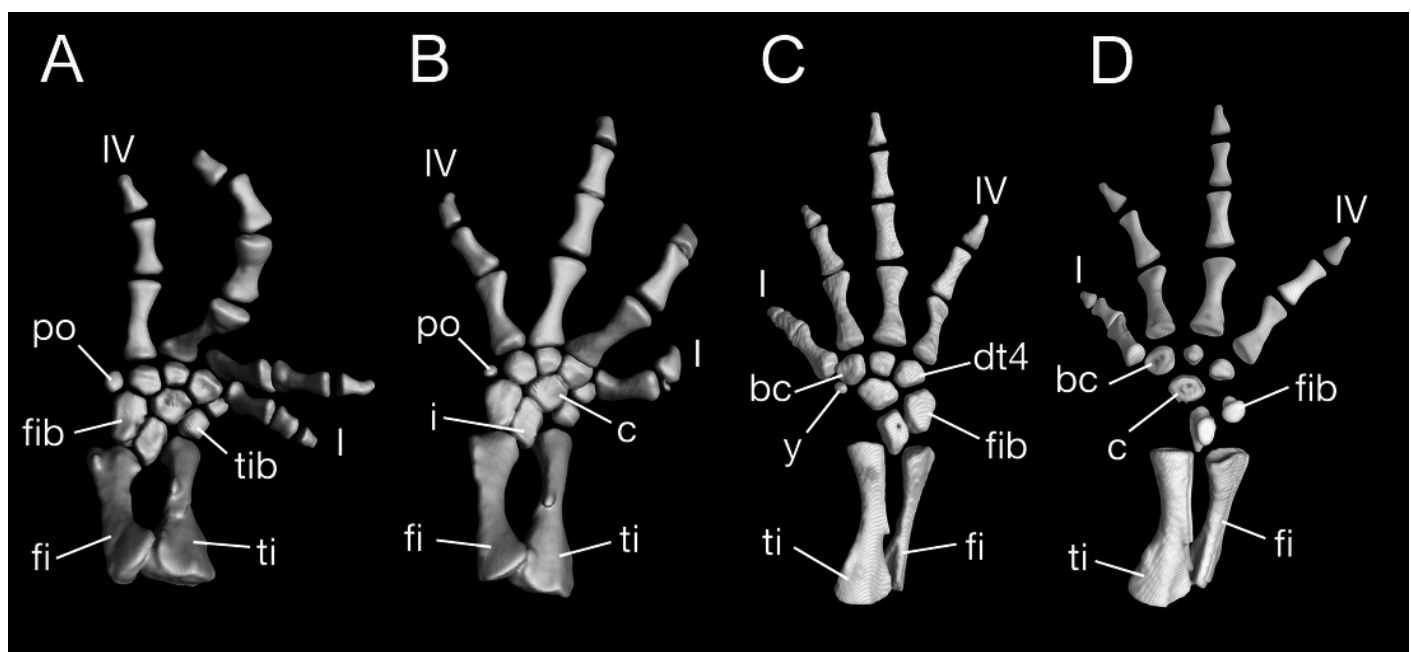
Measurements of specimens used in this study.

Table 1. Measurements of specimens used in this study

(Measurements in mm)

Catalogue Number	Field Number	Male/ Female	External Gill Slits	Total Length	Snout-Pelvic Length	Skull Length	Skull Width
CIB 14500	川 I00202	juvenile	absent	110.07	60.24	16.84	12.82
CIB 14504	65I0012	♀	absent	220.15	117.51	26.96	21.28
CIB 14507	620593	♂	absent	225.35	120.32	34.08	25.69
CIB 14509	638866	♀	absent	219.99	113.15	28.19	23.08
CIB 14380	65I0013	♂	present	265.00	129.00	27.50	23.80
CIB14381	638900	♀	present	221.94	121.00	22.70	20.00
CIB 14482	99I0511	♀	present	178.28	98.10	25.94	17.38
CIB 14484	99I 0517	♂	present	189.05	97.93	26.73	18.35
CIB 14485	99I0520	♀	present	179.39	93.92	25.35	17.77
CIB 14487	99I0513	♂	absent	164.09	89.27	24.38	17.51
CIB 14499	川 I00196	♀	present	214.76	116.96	27.85	21.31